Separation and Purification Technology 346 (2024) 127401

Contents lists available at ScienceDirect

Separation and Purification Technology

journal homepage: www.elsevier.com/locate/seppur

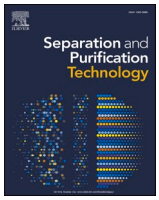

Review

Exploring the membrane-based separation of CO_2/CO mixtures for CO_2 capture and utilisation processes: Challenges and opportunities

Riccardo Checchetto [a], Maria Grazia De Angelis [b,*], Matteo Minelli [c]

[a] Dipartimento di Fisica, Università di Trento, Via Sommarive 14, I-28123 Povo (TN), Italy
[b] Institute of Materials and Processes, School of Engineering, Sanderson Building, EH9 3FB Edinburgh, UK
[c] Department of Civil, Chemical, Environmental and Materials Engineering (DICAM), Alma Mater Studiorum – University of Bologna, via Terracini 28, I-40131 Bologna, Italy

ARTICLE INFO

Keywords:
Gas separation membranes
CO_2/CO separation
Polymers
CO_2 capture, CO_2 utilisation

ABSTRACT

The separation and removal of CO_2 from its mixtures with CO is gaining increasing interest due to the novel processes in which these two gases are mixed, such as the non-thermal plasma activated reaction of CO_2 splitting, a promising CO_2 utilisation route that could be performed using renewable energy. The aim of this review is to propose a novel database suitable for membrane scientists to evaluate the feasibility of membrane-based separation processes involving such gas mixture, not included in the original Robeson's works on the upper bound, nor in later developments. For this reason, we reviewed the data on the permeation, diffusion and sorption of these two gases in different classes of polymers, from polyolefins to polyimides and green polymers, spanning over a wide range of permeability values. Furthermore, we propose an upper bound for this separation, and provide a theoretical explanation for it. The separation mechanism is solubility-driven, and all polymeric membranes inspected in the literature show a CO_2-selective behaviour, despite a very limited, or unfavourable, diffusion selectivity for CO_2, which is consistent with empirical correlations. Consequently, the observed selectivity values are determined by the solubility-selectivity and are comprised mainly in the range 7–20, in agreement with known empirical correlations between the solubility and the critical temperature of the penetrants. Temperature has a detrimental effect on CO_2/CO selectivity, as the activation energy for permeation of CO_2 is always lower than that of CO. In general, while the permeability can vary over several orders of magnitude depending on the polymer nature, selectivity mostly ranges between 7 and 20, which makes the trade-off mechanism between permeability and selectivity rather weak in the case of this mixture. Such an effect provides a wider variety of design choices, and makes this separation attractive for polymeric membranes, if carried out at low temperatures and with CO_2-philic materials. A preliminary calculation of the separation obtainable with single-stage membrane unit for a binary mixture is carried out for some representative polymers.

1. Introduction

In the CO molecule, the carbon atom (C) is connected to the oxygen atom (O) by a triple bond having 0.111 nm length and presenting small dipole moment of 0.122 D [1]. This gas is an important feedstock for the industrial synthesis of different chemicals [2–4], such as: *i*) methanol (CH_3OH) synthesized by CO hydrogenation using the Fischer–Tropsch process [5]; *ii*) phosgene ($COCl_2$) prepared by the $CO + Cl_2 \rightarrow COCl_2$ reaction [6]; *iii*) formic acid ($HCOOH$) produced by a two-step process involving first the reaction of CO with methanol to form methyl formate ($C_2H_4O_2$) and then its conversion to formic acid through reaction with ammonia (NH_3) [7]; and *iv*) acetic acid (CH_3COOH) prepared by means of the Captiva process, where CO and methanol react in presence of a catalyst [8]. CO is used also in food processing where small amounts are added to meat to preserve its red color [9], in medical industry to prepare, for example, aluminum chloride for skin medication [10], and in clinical trials where high purity CO is used as a marker of the respiratory status [11].

CO may be produced by different techniques, some well-established in industry, such as the partial oxidation (POX) of carbon-containing compounds (coal, biomasses or hydrocarbons) and the steam reforming of natural gas. Partial oxidation is carried out in air at very high temperatures and in excess of carbon, and CO formation occurs because the initially produced CO_2 reaches equilibrium with remaining hot

* Corresponding author.
E-mail address: grazia.deangelis@ed.ac.uk (M.G. De Angelis).

https://doi.org/10.1016/j.seppur.2024.127401
Received 29 January 2024; Received in revised form 25 March 2024; Accepted 4 April 2024
Available online 8 April 2024

carbon forming *CO* by the reaction $CO_2(g) + C(s) \rightarrow 2\ CO(g)$ [12]. In steam reforming, natural gas reacts with steam in presence of a Ni catalyst forming a mixture of carbon monoxide and hydrogen [13]. Syngas, as well as reformed gas mixtures, contain also unreacted CO_2 molecules: syngas obtained at $T > 800$ °C by coal POX, for example, has a *CO* content between 30 and 60 vol.% and a CO_2 content between 5 and 15 vol.%, while natural gas steam reforming produces syngas containing about 14 vol.% *CO* and 8 vol.% CO_2 [14]. The *CO* separation from unreformed CO_2 is thus a necessary step prior to the synthesis of fuels and chemicals [14,15]: in methanol production, for example, the CO_2 content of the syngas has to be lower than 4–8 vol.% [15], while in oxo-synthesis the reformed gas has to contain less than 0.5 vol.% CO_2 [16].

An innovative method for POX is plasma reforming: a non-thermal plasma operates at room temperature and atmospheric pressure, generating highly active molecular/atomic species and energetic electrons with 1 to 10 eV energy: when electrons with energy in this interval value collide with CO_2 molecules, they break the $OC = O$ bonds via stepwise vibrational excitation [17,18]. Such innovative process is intensively studied because, when driven by renewable energy, it allows CO_2 recycling with the simultaneous production of *CO* offering a solar-to-fuel efficiency close to 23% [17,18], while the mild reaction conditions are very compatible with subsequent separation via a polymeric membrane.

Current *CO* separation technologies are cryogenic distillation, solvent absorption, adsorption and membrane separation [19,20]. Cryogenic distillation is the dominant technology at industrial level, and two distillation processes have been developed by *Linde Engineering* to separate *CO* from gas mixtures containing H_2: i) low-temperature partial condensation that operates with high pressure gas mixtures having high *CO* and H_2 content and low CH_4 concentration, such as those obtained from partial oxidation; and ii) liquid methane wash that operates with low pressure mixtures having high CH_4 concentration and low CH_4/CO ratio, as those obtained from steam reforming [21]. Cryogenic distillation for *CO* separation is a mature technology producing high purity *CO*: pre-treatments of the gas mixture are needed to remove residual H_2O and CO_2 that could freeze in the cryogenic unit causing clogging problems [19,20]. Absorption separation is based on the different relative solubilities of gas mixture components in a liquid solvent [19]. *CO* absorption only occurs by reversible chemical reactions with the solvent: the industrial COSORB process developed by Tenneco Chemicals, for example, uses the cuprous aluminum chloride ($CuAlCl_4$) complex to selectively capture *CO* in a toluene solution, exploiting the interaction between the *CO* molecule and the $Cu(I)$ metal ion [22]. Absorption for *CO* separation requires lower costs than cryogenic distillation, but the $CuAlCl_4$ complex can be easily poisoned by H_2O and H_2S, thus requiring a pre-treatment process of the gas mixtures to remove them [20], in the same fashion as for cryogenic distillation. Research target for *CO* absorption separation is the synthesis of innovative solvents, such as ionic liquids hosting the metal-complexes selectively adsorbing *CO* [23] or acting themselves as selective *CO* adsorbent [24]. Separation by adsorption process is based on the preferential adsorption of a gas mixture component on a solid surface [19,20,25]. Industrial PSA plants operating for *CO* separation are the COPISA plant by Kawasaki Steel Corporation, where *CO* is separated from BOF gas (basic oxygen furnace gas: volume fractions 71% *CO*, 14% N_2, 13% CO_2, and 2% $O_2 + H_2$) by physisorption in zeolite-based sorbents [26], and the Kobe Steel Ltd plant operating with exhaust gas (68% *CO*, 16% CO_2, 13% N_2, 2% H_2, 1% O_2+ *Ar*, on volume basis) using porous alumina with dispersed copper compounds (*CuCl*, $CuCl_2$) as *CO* chemisorption sites [27]. Adsorption separation is a low-cost technology, but it results convenient when operating with *CO* −rich gases: pre-treatments of the gas mixture are anyway required to remove H_2O and H_2S, which pollute the active adsorption sites [20]. Research aims to develop innovative *CO* sorbent materials easily regenerable with high loading capacity and low cost by improving the performances of traditional sorbents [28] and by developing innovative sorbents made with nano-porous material [29] or metal organic frameworks (MOFs) [30] functionalized with unsaturated transition metal atoms [31] or metal salts [32]. Membranes separate gas components based on difference in their diffusivity and solubility values: applicative interest for membrane separation is due to the low energy consumption, high sustainability and environmentally friendly character [20,33,34]. *CO* separation is used in syngas technology to separate *CO* from H_2 and to change the H_2/CO ratio [35]. Membranes used in industrial plants are typically made of polymeric materials: the PRISM plant by Air System uses polysulfone (PS) hollow fibers membranes [36], while the plant by Toshiba Corporation uses sheet-like cellulose acetate (CA) membranes configured into spiral wound elements [37]. *CO* separation from gases having similar solubility and diffusivity values in polymeric membranes, such as CH_4 and N_2, still remains challenging [20,38]: research efforts are dedicated to the development of facilitated transport membranes made of ionic liquids containing mobile *CO* carriers confined in the pores of a microporous support [39]: examples are 1-hexyl-3-methylimidazolium chloride with *CuCl* as *CO* carrier [40] and 1-ethyl-3-methylimidazolium tetrafluoroborate with $AgBF_4$ as *CO*- carrier [41].

In the scientific literature, many review papers report [42–44] efforts dedicated to the development of polymeric membranes for CO_2 removal such as CO_2/N_2 separation from post-combustion flue gases [45], CO_2/H_2 separation in syngas processing for pre-combustion capture [46] and CO_2/CH_4 separation in natural gas upgrading and biogas sweetening [47]. The need of a tailored design of the membrane material and structure optimized for the specific application is clear. In CO_2/N_2 separation for post-combustion carbon capture, for example, the membrane needs to process large quantities of the flue gas at atmospheric pressure and ambient temperature at CO_2 concentration lower than 14 vol.%: given the small driving force, highly CO_2-permeable and CO_2-selective membranes operating at near ambient conditions are required [48]. Operating conditions for CO_2/H_2 separation in syngas processing are different because the feed typically exhibits a 40 vol.% CO_2 concentration and a 50–60 vol.% H_2 content at temperatures ~ 240 °C and pressures ~ 50 atm: given this large transmembrane pressure available, there is no need for high membrane permeability, but the membrane has to exhibit large CO_2 or H_2 selectivity at high operating temperature [49].

Despite the large interest on CO_2 separation with membranes, however, very few studies dealt with the *CO* transport through polymeric membranes and no review, to the best of our knowledge, focuses on CO_2/CO separation properties and mechanisms. We believe that this mixture deserves special attention due to its peculiar features, such as a very small difference in the diffusion coefficients of the two components, and the presence of a dipole moment in *CO* and of a quadrupolar moment in CO_2 and *CO* that may affect their individual and multicomponent sorption and diffusion behaviors. We will review the experimental information available for such gases in many commercial polymers, in order to identify general trends and provide a theoretical explanation using the most widespread correlations.

2. Theoretical background: Gas transport in polymeric membranes

Gas molecules absorbed in a polymer are hosted in free volume elements (FVE) resulting from the irregular packing of the polymer chains and from local thermal fluctuations of chain segments: transport of penetrant molecules through the polymer layers occurs by successive jumps to adjacent randomly- formed voids [50,51]. The free volume structure of a polymer is empirically described by the fractional free volume (*FFV*) defined as the ratio $(V_{sp} - V_{occ})/V_{sp}$, where V_{occ} is the volume occupied by the polymer macromolecules, and V_{sp} the polymer specific volume, that is the reciprocal of the polymer density ρ [52].

Gas permeation through dense, non-porous polymeric membranes follows the solution-diffusion mechanism: according to this model,

permeant molecules are first dissolved in the polymer layers and then diffuse down to their concentration gradient [53–55]. The gas transport is thus controlled by the penetrant solubility S (practical units: cm^3(STP) cm_{pol}^{-3} $cmHg^{-1}$) and diffusivity D (units: cm^2/s) [53–55].

Gas sorption in polymers depends on temperature as follows:

$$S = S_0 \cdot exp(-\Delta H_S/RT) \tag{1}$$

where the sorption enthalpy $\Delta H_S = \Delta H_C + \Delta H_m$ is given by the sum of ΔH_C (condensation enthalpy of the pure gas to the liquid phase) and ΔH_m (mixing enthalpy of condensed penetrant with the polymer matrix) [53–55]. Penetrant dissolution is indeed as a two-step process, involving first penetrants condensation to a liquid-like density, followed by the mixing of penetrants with the polymer segments.

Experimentally, a strong correlation was observed between parameters measuring the gas condensability such as the Lennard-Jones energy parameter ε/k_B or the critical temperature T_C with vaporization enthalpy $\Delta H_V = -\Delta H_C$, empirically expressed as $\Delta H_V/R = a_c T_c = a_e(\varepsilon/k_B)$, where a_c and a_e are constants. Interestingly, as observed also in experiments on gas solution in liquids, i) for most gases $|\Delta H_m| \ll |\Delta H_C|$; and ii) a_c values in different polymers are quite similar [53–55].

Gas diffusion in polymers is a thermally activated process, so that the D value exhibits an Arrhenius behavior:

$$D = D_0 \cdot exp(-E_D/RT) \tag{2}$$

where D_0 and E_D are the pre-exponential factor and activation energy for diffusion, respectively. Experimentally, it is observed that the gas diffusion coefficient in polymers D increases decreasing the gas molecular size, with the square of a characteristic molecular size d^2 being a pertinent scaling parameter. Such dependence was explained considering that the activation energy for diffusion E_D is proportional to the effective cross-sectional area of the gas molecule [56].

Key operative parameters for a polymeric membrane are the permeability P_i for the generic i gas species and the selectivity α_{ij} for the i,j gas couple. P_i is defined as the flux of a gas through the membrane, divided by its partial pressure gradient $\frac{\Delta p_i}{l}$ (or fugacity gradient, if the gas phase is non ideal)

$$J_i = P_i \frac{\Delta p_i}{l} \tag{3}$$

Considering Fick's law to hold true for the gas in the membrane and a negligible convective flow, the flux is governed by the diffusion coefficient D_i and a concentration gradient $\frac{\Delta C_i}{l}$ across the membrane, as follows:

$$J_i = D_i \frac{\Delta C_i}{l} \tag{4}$$

Now assuming that there is equilibrium at the gas/polymer interface, according to which concentration and partial pressure are related through the incremental solubility coefficient S_i

$$S_i = \frac{\Delta C_i}{\Delta p_i} \tag{5}$$

the permeability can be seen as the product of gas solubility and diffusivity

$$P_i = D_i S_i \tag{6}$$

and it provides a measure of the membrane productivity: in stationary transport conditions, in fact, the permeation flux J_i of the i gas species through a polymeric membrane of thickness l is given by the relation

$$J_i = \frac{D_i}{l} S_i \Delta p \tag{7}$$

where Δp is the *trans*-membrane pressure. In the SI system, permeability units are mol/m s Pa, but its values are commonly reported in Barrer (1 Barrer $= 10^{-10}$ cm^3 (STP) cm/cm^2 s cmHg $= 3.35 \cdot 10^{-16}$ mol/m s Pa): permeability values depend on the specific polymer-gas couple and operative conditions (T, p and composition), and span over several orders of magnitude [32–34].

The gas transport through polymeric membranes is a thermally activated process and the relation between gas permeability P and temperature T can be expressed as

$$P = P_0 exp(-E_P/RT) \tag{8}$$

where E_P is the effective activation energy for permeation which is given by $E_P = E_D + \Delta H_S$ [53–55]. While the E_D term is always positive, the sign of E_P may depend on the values of E_D and ΔH_S: the net gas transport rate thus increases with temperature when $E_D > |\Delta H_S|$, otherwise it decreases [53–55].

The membrane selectivity α_{ij} for the i,j gas couple, when the downstream pressure is negligible with respect to the upstream one, reduces to the ratio of the gas permeability of gas i to the permeability of gas j:

$$\alpha_{ij} = \frac{P_i}{P_j} = \left(\frac{D_i}{D_j}\right)\left(\frac{S_i}{S_j}\right) \tag{9}$$

α_{ij} can be thus portioned into diffusivity- selectivity, $\alpha_{ij}^D = \left(\frac{D_i}{D_j}\right)$, and solubility-selectivity $\alpha_{ij}^S = \left(\frac{S_i}{S_j}\right)$ [32–34]. For the sake of simplicity, the α_{ij} values are often determined from permeability measured in single gas tests, and in that case the selectivity is referred as "ideal". For any given polymer, the α_{ij} value depends on the specific gas couple: in polysulfone (PSF) dense films, for example, the ideal selectivity decreases from $CO_2/CH_4 = 23$ to $CO_2/O_2 = 4$ and to $CO_2/He = 0.4$ [53–55].

Applications require polymers with high permeability to decrease the membrane surface area to separate a given feed flow rate of gas, and high selectivity to improve the purity of the separated gas. The large amount of literature about polymeric membranes for gas separation evidence that an empirical trade-off exists between permeability and selectivity for any i,j gas couple: polymers exhibiting high selectivity values are generally less permeable and *vice-versa*. Such trade-off, called Robeson limit, can be described as an upper-bound, where all permeability-selectivity data in log–log scale are below an empirical line [57,58]. The Robeson upper bound is quantitatively described by the line:

$$\alpha_{ij} = \frac{\beta_{ij}}{P_i^{\lambda_{ij}}} \tag{10}$$

which indicates that, as the permeability to a gas i of an upper bound polymer P_i increases, the selectivity α_{ij} of the polymer for gas i over gas j decreases. Empirically obtained values for the λ_{ij} parameter (slope of the upper bound line) and β_{ij} parameter (position of the upper bound line) for different gas couples were reported by Robeson [59].

Freeman presented a model able to predict the λ_{ij} and the β_{ij} parameters for a given gas pair. According to this model, the λ_{ij} parameter depends on the kinetic diameters of the gas molecules d_i and d_j, while the β_{ij} parameter is related to their solubility values S_i and S_j:

$$\lambda_{ij} = \left(\frac{d_j}{d_i}\right)^2 - 1 \tag{11}$$

$$\beta_{ij} = \left(\frac{S_i}{S_j}\right) S_i^{\lambda_{ij}} exp\left\{-\lambda_{ij}\left[b - f\left(\frac{1-a}{RT}\right)\right]\right\} \tag{12}$$

In eq. (12), the values of a and b are independent of the gas type; the b parameter depends on the polymer class (e.g. rubbery or glassy) while the a value is universal for all polymers. The f parameter changes with the equilibrium inter-chain spacing increasing from rubbery to glassy polymers [60].

3. Data review

3.1. Polyolefins

Polyolefins are semi-crystalline polymers with general formula $(CH_2CHR)_n$, where R is an alkyl group, made from alkene monomers through addition polymerization [61]. Polyethylene is the most widely produced thermoplastic polymer, and it finds applications mostly in packaging. Michaels and Bixler studied the permeation of light gases through different polyolefin films to analyze the relation with the crystalline degree: to this task, they examined samples produced by different companies: *i*) Grex which is a linear polyethylene with 23 vol.% amorphous fraction; *ii*) Alathon 14, a branched polyethylene with 57 vol.% amorphous fraction; *iii*) Hydropol, a hydrogenated polybutadiene (71 vol.% amorphous fraction); and *iv*) un-vulcanized fully amorphous natural rubber [62]. Single gas permeation tests were carried out in dead-end configuration using polymer film membranes 0.024 to 0.178 cm thick, in the temperature range from 5 to 55 °C at feed pressure values p_{feed} up to ~ 1 bar. Obtained results are reported in Table 1. Results indicated that the membrane films with higher crystalline degree (Grex) exhibited the lowest *CO* and CO_2 transport rates and resulted poorly selective: the ideal CO_2/CO selectivity value was, in fact, ~ 1.9, nearly equal to the CO_2/CO diffusivity ratio of 1.3. The CO_2 and *CO* gas transport rates, as well as the CO_2/CO selective properties, improved increasing the amorphous fraction of the samples: the ideal CO_2/CO selectivity values of other polyolefin samples were, in fact, between 8.5 and 9.8. The authors also observed that the CO_2/CO diffusivity ratio was ~ 1, as in the nearly crystalline one, evidence that the ideal CO_2/CO selectivity of the samples with larger amorphous fraction exhibited solubility selective character. Increasing temperature, the CO_2 and *CO* transport rates increased but the CO_2/CO selectivity decreased. Activation energies values for CO_2 (*CO*) permeation ranged from 21.7 (30.9) for Grex to 38.9 (46.4) kJ/mol for Alathon, while E_D for CO_2 (*CO*) diffusion ranged from 34.3 (30.89) for Grex to 38.5 (39.7) kJ/mol for Alathon. The permeability of both gases is strongly affected by crystallinity: indeed, it increases by around 2 orders of magnitude with the amorphous fraction, and more markedly for CO_2 than for *CO*. Gas transport, indeed, is not expected to occur in the crystalline phase, but only in the amorphous region; such feature dictates the permeability to scale at least quadratically with the amorphous fraction [63], although the crystallites may depress gas solubility even further [64]. The selectivity also increases, although less markedly, with the amorphous content. This is partly due to the fact that the diffusion-basedselectivity decreases with the amorphous fraction, from 1.29 to 0.93.

In synthesis, for polyolefins: *i*) films of different crystallinity are moderately CO_2-selective, with ideal CO_2/CO selectivity values always lower than 10; *ii*) CO_2 permeability increases by two orders of magnitude with the amorphous fraction, spanning from 0.36 to 154 Barrer, while the selectivity increases moderately; *iii*) the CO_2/CO separation is governed by solubility, as the D_{CO_2}/D_{CO} value is ~ 1.

If one of the hydrogen atoms is substituted by a *Cl* atom, we obtain **polyvinyl chloride** (PVC), which, compared to polyethylene, has higher hardness and stiffness due to the *Cl* atoms increasing the inter chain attraction. Sefcik *et al.* carried out a study on the H_2 and *CO* transport through PVC films prepared by solution casting method adding tricresyl phosphate (TCP) as plasticizer/anti-plasticizer agent, and examined how the changes in the polymer structure affected the penetrant transport rates [65]. The authors carried out measurements at 27 °C and 3.6 bar feed pressure, and observed that the H_2 and *CO* permeability and diffusivity values slightly decrease increasing the TCP content up to 15 wt.%, then start to increase strongly, see Table 2. The P_{CO} of the neat PVC films (0.025 Barrer) increased to 0.37 Barrer in PVC film with 40 wt.% TCP. The D_{CO} value was of 2.3 to 2.5 $\times 10^{-9}$ cm^2/s in the 0 to 15 wt.% additive content and raised by a factor 10 in the samples containing 40 wt.% plasticized. The CO_2 permeability value of neat PVC films was found from other literature works. Brubaker and Kammermeyer studied the H_2 and CO_2 transport properties of commercial Polyone GeonTM 101-EP-100 PVC films from Goodrich Co and found a P_{H_2} value of 3.5 Barrer at 30 °C which is compatible with the value obtained by Sefcik *et al.* (2.38 Barrer) and a P_{CO_2} value of 1.02 Barrer [66]. The CO_2 transport properties of neat PVC films prepared by solution casting method were measured also by Tiemblo *et al.*, which obtained at 1 bar feed pressure and 25 °C a P_{CO_2} value of 0.54 Barrer and a D_{CO_2} value of 0.104 $\times 10^{-8}$ cm^2/s [67] while Yeon *et al.* reported a value of 1.69 Barrer at 35 °C and 2 bar feed pressure using a CO_2/N_2 gas mixture [68]. The effect of TCP addition to the CO_2 transport properties of PVC films was studied by Ballard et al. which reported an increase of the P_{CO_2} value from 0.67 Barrer for the neat film to 0.85 Barrer with 10 wt.% plasticized addition [69].

Comparing the above reported experimental information the following conclusions can be drawn: *i*) PVC film are CO_2-selective with ideal CO_2/CO selectivity values higher than ~ 20; *ii*) the CO_2 permeability is always lower than 1.45 Barrer at room temperature but it can be increased adding plasticizers; *iii*) the D_{CO_2}/D_{CO} value of PVC is ~ 0.4.

3.2. Polyimides

Polyimides (PI) are commercial high-performance engineering thermoplastics containing the imide group $-C=ONC=O-$ synthesized by condensation reaction of a dianhydride with a diamine. Given their high thermal resistance and good mechanical properties at high temperature, PIs are used for demanding applications in electronic industry, e.g. as insulating films in magnetic wires or passivation layers in integrated circuits and in mechanical industry to produce bushings, bearing and sockets [70]. Among them, aromatic PIs are of particular interest as membrane materials because of their excellent physical–chemical properties and high permeability/selectivity: applications are envisaged in the separation of polar/polarizable components of a gas mixture, given the affinity of polar imide groups with electrons of polar components of the mixture [71]. Unfortunately, PIs presents high manufacturing costs and their application as membrane material are limited by the low processability and limited solubility in organic solvents caused by the so-called charge transfer complex (CTC) which inhibits the macromolecular mobility and narrows the intersegmental distance [70]. The incorporation of ester, amide, flexible groups such as $-CH_2$, $-SO_2$ and bulky groups as $-CF_3$, into the polymer backbone permits to control the macromolecular chain packing, the polymer free volume and the penetrant solubility. PIs containing the 6FDA group, for example, have shown the highest CO_2 permeability values and their high CO_2/N_2 selectivity was attributed to the chain packing effectively separating molecules based on their steric bulk [71].

Tanaka *et al.* studied the gas transport properties of solution-cast

Table 1
CO_2 and *CO* single gas permeability (P) and diffusivity (D) values in polyolefin films [62]. α: ideal selectivity, α_D: diffusivity- selectivity, α_S: solubility-selectivity.

Polymer	T (°C)	P_{CO2} (Barrer)	D_{CO2} (cm^2/s)	P_{CO} (Barrer)	D_{CO} (cm^2/s)	α	α_D	α_S
PE (Grex)	25	0.36	1.2×10^{-7}	0.19	0.96×10^{-7}	1.87	1.29	1.45
PE (Alathon 14)	25	12.6	3.7×10^{-7}	1.49	3.3×10^{-7}	8.46	1.12	7.6
Hydropol	25	48.2	9.1×10^{-7}	6.18	8.2×10^{-7}	7.80	1.11	7.0
Natural rubber	25	154	12.5×10^{-7}	15.8	13.5×10^{-7}	9.75	0.93	10.2

Table 2
CO_2 and CO single gas permeability (P) and diffusivity (D) values in neat PVC and PVC-TCP thin films. α: ideal selectivity, α_D: diffusivity- selectivity, α_S: solubility-selectivity. Selectivity values in row 5 for neat PVC film were calculated using refs. [67] and [66] for CO_2 and [65] for CO; for the neat and plasticized film in row 6 using ref. [69] for CO_2 and [65] for CO. Experimental tests in refs. 65 and 68 were carried out at fixed permeant pressure by constant-volume variable-pressure method, in refs. 66 and 69 by variable-volume constant-pressure method, in ref. 67 in mixed gas conditions using a commercial permeation apparatus.

polymer	T (°C)	P_{CO2} (Barrer)	P_{CO} (Barrer)	D_{CO2} (cm^2/s)	D_{CO} (cm^2/s)	α	α_D	α_S
PVC [66]	30	1.02	–	–	–	–	–	–
PVC [67]	25	0.54	–	1.04×10^{-8}	–	–	–	–
PVC [68]	35	1.69	–	–	–	–	–	–
PVC [65]	27	–	0.025	–	2.3×10^{-9}	22	4.5	4.9
PVC + 5 wt.% TCP		–	0.015	–	2.1×10^{-9}	–	–	–
PVC + 15 wt.% TCP		–	0.018	–	2.5×10^{-9}	–	–	–
PVC + 20.1 wt.% TCP		–	0.027	–	2.9×10^{-9}	–	–	–
PVC + 30.8 wt.% TCP		–	0.11	–	5.4×10^{-9}	–	–	–
PVC + 40 wt.% TCP		–	0.37	–	2.9×10^{-8}	–	–	–
PVC [69]	35	0.67	–	–	–	27	–	–
PVC + 5 wt.% TCP		0.68	–	–	–	43	–	–
PVC + 10 wt.% TCP		0.85	–	–	–	50	–	–

amorphous PI films by gas-phase permeation tests carried out in single gas conditions using H_2, CO, CO_2 and CH_4 at 10 bar feed pressure and temperatures between 25 and 110 °C. In a first study, the authors prepared PIs films using **BPDA** (3,3′,4,4′-biphenyltetracarboxylic dianhydride) and **ODA** (4,4′-oxidianiline, $O(C_6H_4NH_2)_2$) units, and annealed the prepared samples under different conditions to examine the correlation between transport properties and specific volume [72]. Experimental results indicated that the CO_2 and CO permeability of the prepared samples, as well as the CO_2 diffusivity value, decreased with the PI specific volume without showing relevant variations of the CO_2/CO selectivity value. At 50 °C the CO_2/CO selectivity was ~ 13 and the D_{CO_2} and D_{CO} diffusivity values were nearly equivalent, 2.1×10^{-9} cm^2/s for CO and 2.53×10^{-9} cm^2/s for CO_2, evidence that the CO_2/CO selective properties are conferred by solubility. Decreasing the specific volume of the samples, the activation energy value for CO_2 permeation and diffusion increased while only minor variations were observed in the CO_2 sorption enthalpy. No data were reported on the CO transport at temperatures different from 50 °C. The authors attributed the observed increase of gas permeability to the amount of amorphous phase fraction resulting from different annealing conditions [72].

In a subsequent study, the authors prepared amorphous polyimide films using **BPDA** and symmetrical aromatic diamines having different structures, namely **ODA**, **MDA** (4,4′ −methylenedianiline with formula $CH_2(C_6H_4NH_2)_2$), **DDS** (4,4′ −diaminodiphenil sulfone with formula $CH_2(C_6H_{10}NH_2)_2$ and **DDBT** (dimethyl-3,7-diaminodibenzotriophene 5,5′ –dioxide) [73]. The latter one is a mixture of isomers having methyl groups bonded at different positions of the aromatic ring namely 63% at 2,8-, 33% at 2,6, and 4% at 4,6-positions). At 50 °C in single gas tests with 10 bar feed pressure, they observed that the CO_2 and the CO permeability values scaled in the following order: BPDA-DDBT > BPDA-DDS > BPDA-MDA > BPDA-ODA: the authors hypothesized that the increase of the rigidity and bulkiness of the polymer backbone reduces the chain packing and produces more open structures, facilitating the penetrant transport. In fact, the activation energy for CO_2 permeation decreased from 16.1 kJ/mol for BPDA-ODA to 6.7 kJ/mol for BPDA-DDBT, the activation energy for diffusion decreased from 34.3 to 23.2 kJ/mol while no relevant variation was observed for the CO_2 heat of solution, −17 kJ/mol. No data were reported for the CO transport at temperatures different from 50 °C. The CO_2/CO selectivity value of the BPDA-DDS, BPDA-MDA and BPDA-ODA films was ~ 13 and increased to ~ 17 for the BPDA-DDBT film with nearly equivalent diffusivity values for CO_2 and CO [73].

The authors then investigated the gas transport properties of a series of **fluorinated** and non-fluorinated amorphous PI films, looking for the correlation between chemical structure and gas selectivity [53]. To this aim they used PI made with four tetra carboxylic dianhydrides: 1) 1,2,3,5-benzenetetracarboxylicanhydride (**PMDA**), 2) **BPDA**, 3) benzophenone-3,3′,4,4′-tetracarboxylic dianhydride (**BTDA**) and 4) 2,20-bis-(3,4-dicarboxylphenyl) hexafluoropropane dianhydride (**6FDA**) and six diamines: 1) 2,2-bis- (4-aminophenyl) hexafluoropropane (**BAHF**), 2) 2,2-bis (4- (4-aminophenoxy) phenyl)- hexafluoropropane (**BAPHF**), 3) 2,2-bis (4- (4-amino-2-trifluoromethylphenoxy) phenyl)- hexafluoropropane (**BATPHF**), 4) 4,4′-oxydianiline (**pp'ODA**), 5) 3,4′-oxydianiline (**mp'ODA**) and 6) 2-(3-amino-phenyl)-2-(4-aminophenyl)propane (**APAP**). They observed that the obtained PIs exhibited CO_2 and CO permeability increasing with the fluorine group concentration and attributed the improved transport rates to the lower packing of the polymer chains. According to their measurements, at 35 °C and 10 bar feed pressure, polyimides with the 6FDA anhydride and/or the BAHF diamine exhibited the highest CO_2 permeability, ranging from 6 Barrer for 6FDA-mp'ODA with CO_2/CO selectivity ~ 12 to 51 Barrer for 6FDA-BAHF with CO_2/CO selectivity value ~ 15. In all examined polymer films, the CO_2/CO couple shows a favorable D_{CO_2}/D_{CO} ratio ~ 2 [74].

Tanaka *et al.* finally investigated the gas transport properties of PI films prepared using the 6FDA anhydride and methyl substituted phenylene diamines to examine the effect of the methyl-substitute in the diamine [75]. To this task, the authors used 1,3-phenylenediamine (**mPD**), 1,4-phenylenediamine (**pPD**), 2-methyl-1,3-phenylenediamine (**mMPD**), 2,5-dimethyl-1,4-phenylenediamine (**pDiMPD**), 2,5-trimethyl-1,4-phenylenediamine (**mTrMPD**) and 2,5-tetramethyl-1,4-phenylenediamine (**pTeMPD**). The aim was to manipulate the polymer chain packing by inserting the bulky methyl groups restricting the internal rotation around the bonds between phenyl and imide. This route permitted to greatly increase the penetrant permeability at expenses of a reduced CO_2/CO selectivity, which was lower than 12 [75].

Graphs of the CO_2 and CO permeability and diffusivity values as a function of the inverse fractional free volume ($(FFV)^{-1}$) of the PI films are shown in Fig. 1. Using P and D data there reported we evaluated the ideal CO_2/CO selectivity and CO_2/CO diffusivity selectivity which are shown in Fig. 2. The *FFV* values in these figures are obtained from refs. 52–54 and were calculated by the authors using the Bondi's method. The correlation of CO_2 and CO permeability with the PI film density is reported in fig. A of the Supplementary Information Section.

Looking at Figs. 1 and 2 it can be said that, while the diffusivity decreases with increasing inverse *FFV*, the permeability seems less correlated to it, which further indicates that the CO_2/CO separation is not driven by a sieving mechanism. The effect of FFV on both gases is similar, so that ideal selectivity as well as the diffusivity selectivity are independent on the *FFV*.

Park *et al.* prepared a series of innovative semi-alicyclic aromatic polyimides by one-step thermal solution imidation in *m*-cresol using an alicyclic dianhydride with non-planar twisted structure 5-(2,5-dioxotetrahydrofuryl)-3-methyl-3-cyclohexene-1,2-dicarboxylic anhydride

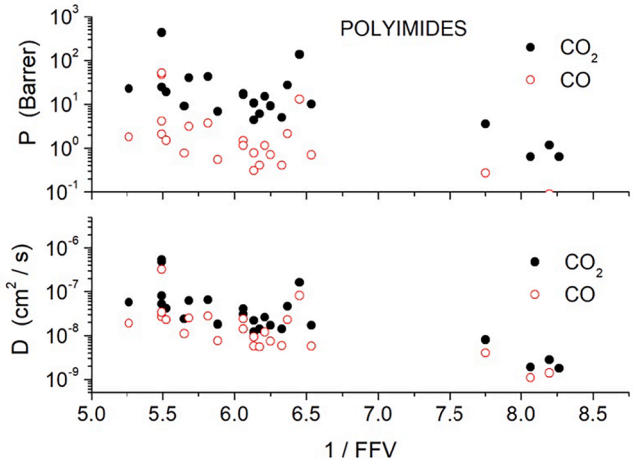

Fig. 1. CO_2 and CO permeability and diffusivity values as a function of the inverse fractional free volume $(FFV)^{-1}$ of the PI films [73–75].

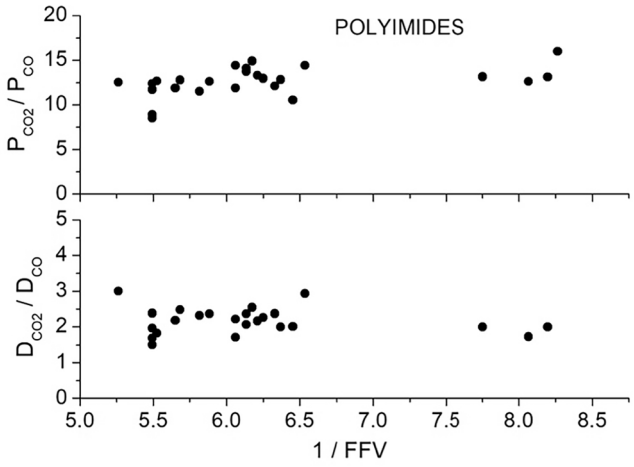

Fig. 2. Ideal CO_2/CO selectivity and CO_2/CO diffusivity selectivity as a function of the inverse fractional free volume $(FFV)^{-1}$ of the PI films [74,75].

(**DODCA**) and five aromatic diamines (**pDPDA**, **BAPF**, **MDA**, **ODA** and **pPDA**) [76]. Dense membrane films were then prepared by solution casting using DMF (N,N-dimethyl methanamide) as solvent. The permeability of 50–60 μm thick samples at 25 °C to H_2, CO_2, O_2, CO, N_2 and CH_4 was studied by time-lag method with pure gas at 2.7 bar in the upstream side. The authors observed that all examined samples were CO_2- selective and that the CO_2 permeability followed the order DOCDA-pDPDA > DOCDA-BAPF > DOCDA-MDA > DOCDA-ODA > DOCDA-pPDA. Results evidenced a clear correlation between the polymer fractional free volume as evaluated by Bondi's method and the CO_2 transport rates. The authors attributed the higher permeability and lower selectivity of the DOCDA-pDPDA and DOCDA-BAPF to the presence of the bulky cardo structure of BAPF and the two methyl substituents of the pDPDA structure, which disrupt the chain packing and increase the sample *FFV* at expenses of a lower selectivity [76].

Various commercially available polymeric membranes for gas separations are based on a polyimide chemistry [77], often using proprietary materials not fully disclosed. As reference polymers, in the field of CO_2 separation for various applications, the following commercial polyimides are considered as benchmark.

Upilex® is the commercial name of polyimide film produced by Ube Industries Ltd. by polycondensation reaction starting from the biphenyl tetracarboxylic dianhydride (BPDA) monomer exhibiting molding processability. Tanaka *et al.* carried out gas-phase permeation tests in single gas conditions at 10 atm feed pressure and temperatures between 25 and 110 °C using the Upilex® as a standard: they found a P_{CO_2} value of 0.16 Barrer and P_{CO} value of 0.012 barred indicating a CO_2/CO selectivity ~ 13. The P_{CO_2} value is compatible with the value of 0.46 Barrer reported by the Upilex® technical sheet [78]. The measured D_{CO} value of 0.7×10^{-9} cm^2/s resulted nearly equivalent to the D_{CO_2} value of 0.84×10^{-9} cm^2/s, indicating that the CO_2/CO selectivity is mostly given by solubility [72].

Matrimid® is a commercial PI with good solubility in most organic solvents which exhibits high CO_2 selectivity and acceptable transport rates. Matrimid® has a glassy structure, and it is obtained by polycondensation of 3,3′,4,4′-benzophenone tetracarboxylic dianhydride (BTDA) and a mixture of two rigid cycloaliphatic indane-type monomers, 5- and 6-amino-1-(4′-aminophenyl)-1,3,3-trimethylindane. Matrimid® exhibits high chemical resistance that permits its use for the upgrade of biogas and natural gas [79]. The properties of dense Matrimid® films prepared by solution casting method using Matrimid 5218 powders (Huntsman Advanced Polymers) and dichloromethane as solvent were studied by Checchetto *et al.* in a dead-end configuration testing the permeation of CO_2, CO, N_2 and O_2 in single and mixed gas conditions with feed pressure up to 1 bar and temperatures between 25 and 80 °C [80]. At 25 °C, the Matrimid® membrane exhibited CO_2 and CO single gas permeability values of 8.1 and 0.5 Barrer, respectively, with ideal CO_2/CO selectivity ~ 16. Increasing temperature, the transport rates of both penetrants increased, but the CO_2/CO selectivity decreased: at 62 °C, in fact, the P_{CO_2} and P_{CO} values were 11.1 and 1.14 Barrer, respectively, and the ideal CO_2/CO selectivity decreased to ~ 10. No marked variations of gas permeability and selectivity values were observed exposing the membrane sample to ternary ($CO_2/CO/O_2$) and quaternary ($CO_2/CO/O_2/N_2$) gas mixtures, evidencing that, in the low pressure region inspected, neither competitive sorption nor plasticization phenomena occur. The analysis of the permeation process revealed slightly larger diffusivity values for CO than for CO_2, 3.9×10^{-9} and 2.2×10^{-9} cm^2/s, indicating that the system has solution-selective behavior. The activation energy values for CO_2 (CO) permeation and diffusion were 7.7 (20.7) and 32.5 (28.7) kJ/mol.

Similar results were obtained by David *et al.* in a study on the H_2 recovery from post-combustion gases using a Matrimid® 5218 prepared by solution-casting method with CH_2Cl_2 as solvent [81]. At 30 °C and 2 bar feed pressure in single gas tests the authors found a P_{CO_2} value of 6.4 Barrer and a P_{CO} value of 0.45 Barrer indicating a CO_2/CO selectivity of ~ 14. The P_{CO_2} values slightly decreased increasing the CO_2 feed pressure, going to 5.4 at 4 atm, while no change was observed on the P_{CO} value. Increasing the temperature, the CO_2 and CO transport rates increased: the authors obtained values of 8.1 and 16.5 kJ/mol for the activation energy of CO_2 and CO permeation, respectively. The CO_2/CO selectivity thus decreased with temperature, reaching the value ~ 10 at 100 °C. In mixed gas tests, the CO_2 transport rates was unaffected by the presence of CO. In this study, no information was reported on the CO_2 and CO diffusivity values [81].

Kapton® is the commercial name of DuPont polyimide produced from the condensation of pyromellitc acid (PDMA) and 4,4′-oxydiphenylamine (ODA), offering high thermal stability in a wide temperature range. The CO permeability value of Kapton® films was measured by McCandless [82], and its value increased from 0.027 Barrer at 30 °C to 0.14 Barrer at 100 °C with *trans*-membrane pressure up to 3.5 bar. The CO_2 permeability of Kapton® polyimide was measured by Hausladen *et al.* using 75 μm thick dense films to test the high temperature separation performances for mixtures produced by partial oxidation of methane [83]. Measurements were carried out at 0.67 bar feed pressure in dead end configuration: at 50 °C, the authors measured a P_{CO} value of 0.023 Barrer well compatible with the value of McCandless, and P_{CO_2} equal to 0.51 Barrer: their measurement thus indicate a CO_2/CO selectivity of 22 at 50 °C and of 8 at 150 °C. In the 50 to 250 °C temperature range, the authors evaluated E_P values for CO_2 (CO)

permeation of 17.4 (28.4) kJ/mol.

Polyetherimide (PEI) is an amorphous thermoplastic co-PI that exhibits the strength, heat resistance and flame retardancy of traditional polyimides (PIs) with the ease of simple melt processing [84]. In PEI membranes the CO_2- philic ether functional groups improve the CO_2 solubility, as well as the flexibility of polymer chains [84]. Ultem® is a commercial PEI produced by Sabic Co. containing flexible ether linkages with fluorinated groups. Hamidavi *et al.* reported recently the transport of syngas mixtures ($H_2/CO/CO_2$) through nanocomposite Ultem 1000 polyetherimide films prepared by solution-casting method using N-methyl-2-pyrrolidone as solvent [85]. Permeation tests were carried out in single gas conditions at feed pressure from 2 to 6 bar using a variable feed pressure/constant volume method. The obtained permeability value for CO_2 and CO at 25 °C were 0.3 and 0.05 Barrer, respectively, indicating a CO_2/CO selectivity near 6. Their measurements indicated a D_{CO} value in the 10^{-9} cm^2/s order and D_{CO_2}/D_{CO} diffusivity ratio ~ 1.5. The activation energy value for CO_2 and CO permeation in the net PEI films were evaluated in the 25 to 55 °C interval to be 34.7 and 78.7 kJ/mol, respectively. The authors also prepared nanocomposite samples dispersing hydrophobic fumed silica nanoparticles up to 20 wt.% content (SiO_2 by AEROSIL® R974). They found that at 5 wt.% filler, the CO_2 and CO permeabilities increase with respect to those of the neat PEI film without variations of the CO_2/CO selectivity. Increasing the filler content, the permeability values decrease and become lower than those of the neat film but the CO_2/CO selectivity increases: at 20 wt.%, for example, P_{CO_2} and P_{CO} values are 0.17 and 0.0128 Barrer, respectively, with CO_2/CO selectivity value ~ 13 [85].

Checchetto *et al.* studied the gas transport of $CO_2/CO/O_2/N_2$ ternary and quaternary gas mixtures through polyetherimide films prepared by solution-casting using PEI pellets (Sigma –Aldrich, Milan) and $CHCl_3$ as solvent. Test were carried out in single gas and mixed gas conditions at sub-atmospheric pressure in the 25 to 70 °C temperature interval. The authors found that CO_2 and CO transport obeyed to the solution-diffusion model with permeability values at 25 °C of 1.17 and 0.07 Barrer, respectively. The obtained CO_2/CO selectivity value ~ 16 has sorption-driven behavior, being the CO_2 and CO diffusivity values comparable, 8.5×10^{-9} and 1.08×10^{-8} cm^2/s, respectively. The activation energy for CO_2 permeation was 1 kJ/mol while the corresponding value for CO was 9.3 kJ/mol; nearly equivalent values were obtained for the CO_2 and CO activation energy for diffusion, 20.0 and 21.9 kJ/mol, respectively. Increasing temperature, the P_{CO2}/P_{CO} selectivity values decreased from ~ 16 at 20 °C to ~ 10 at 70 °C, while D_{CO_2}/D_{CO} remained around ~ 0.7 [80].

To summarize: *i*) Polyimides show rather variable values of CO_2 permeability, ranging from 0.09 to 440 Barrer, depending on the chemical and physical nature of the materials, in particular P_{CO_2} increases with fluorination and free volume; *ii*) The CO_2/CO selectivity, on the other hand, is quite constant, with an average value of 13.4 and standard deviation limited to 2.9; *iii*) The activation energy for CO_2 permeation is lower than for CO, indicating a detrimental effect of temperature on the separation,

3.3. High permeability polymers

Polydimethylsiloxane (PDMS) is an organosilicon compound with chemical formula $CH_3\left[Si(CH_3)_2O\right]_nSi(CH_3)_3$ and it is the most employed membrane material for the separation of organic vapors from permanent gases. The backbone of this rubbery polymer ($T_g < -100$ °C) is formed by $Si-O$ units giving it high flexibility. It exhibits density $\rho \sim 1$ g/cm^3 with a large fractional free volume, $FFV \sim 0.18$ which consists of a bimodal hole- size distribution centered at ~ 0.20 and 0.39 nm with poor ability to select molecules based on their size; its selectivity is thus controlled by differences in penetrant solubility [86].

Poly(1-trimethylsilyl-1-propyne) (PTMSP) is a substituted polyacetylene containing bulky trimethylsilyl side groups in a rigid backbone chain resulting in a super-glassy hydrophobic polymer having density $\rho \sim 0.75$ g/cm^3 with a very large fractional free volume, $FFV \sim 0.343$. Its free volume structure exhibits a bimodal hole size distribution centered at 0.45 and 0.75 nm. In PTMSP free volume holes are interconnected forming nanochannels between packed polymer chains through which penetrant transport occurs. The free volume structure of this glassy polymer ($T_g > 300$ °C) impedes to select molecules based on their size and, despite its glassy character, the PTMSP selectivity is attributed to competitive solubility effects: higher hydrocarbons enter accessible cavities, preventing lesser condensable gases from diffusing through the blocked channels [87]. PDMS membranes as well as PTMSP membranes have thus found applications in membrane-based vapor separation processes [88].

Polyether block amine (PEBA) is a thermoplastic elastomer made of soft polyether blocks and rigid polyamide blocks produced by polycondensation of a carboxylic acid polyamide and an alcohol terminated polyether: the manipulation of these building blocks permits the formation of polymers with a wide range of flexibility and impact resistance and is thus used to replace common elastomers such as polyurethanes and silicones.

Pebax® is the commercial name of PEBA produced by Arkema: it is a block copolymer consisting of soft PEO segments acting as gas permeable phase and hard PA segments which impart the mechanical stability exhibiting large fractional free volume: calculation based on Bondi group method suggest that Pebax®-1657 (60 wt.% PEO, 40 wt.% PA) exhibits FFV value ~ 0.15 [89]. PALS analyses on PEBAX®-1657 suggest a FFV value 0.12, compatible with the theoretical value, and revealed that the free volume structure consists of voids with ~ 0.32 nm average size [90,91].

Wilks and Rezac studied the H_2S, CO, CO_2 and H_2 transport properties of **PDMS** films to evaluate their ability in the separation of mixtures obtained in the conversion of organic compounds by reaction with steam or oxygen (gasification gases). They prepared 500 μm thick PDMS films and carried out permeation tests with a constant volume/variable pressure apparatus at temperatures up to 200 °C with 10 bar feed pressure in single and mixed gas conditions. At 35 °C, the examined PDMS membrane were CO_2−selective, with ideal CO_2/CO selectivity values of ~ 8 and permeability of 3700 Barrer for CO_2 and 440 for CO. In the 35 to 200 °C temperature range, the activation energy for permeation in PDMS was −2.4 kJ/mol for CO_2 and 7.8 kJ/mol for CO, indicating a worsening of the CO_2/CO separation performances with temperature ($\alpha \sim 3$ at 100 °C) [92].

Merkel *et al.* studied the transport of simulated syngas mixture (42 vol.% H_2 − 46 vol.% CO − 10.5 vol.% CO_2 − 1.5 vol.% H_2S) through 15 μm thick PDMS films supplied by Membrane Technology and Research, Inc. (Menlo Park, CA). Tests were carried out from room temperature to 240 °C using a constant pressure/variable volume apparatus equipped with a gas chromatograph (GC). At $T = 23$ °C and 1.4 bar feed pressure the authors found a P_{CO} value of 500 Barrer with CO_2/CO selectivity value of 6.4. Activation energy for CO_2 and CO permeation in the examined temperature interval was 2.2 and 11 kJ/mol, respectively. The CO_2/CO separation performances decreased with temperature: at 150 °C the CO_2/CO selectivity was, in fact, ~ 2 [93].

Wilks and Rezac also studied the H_2S, CO, CO_2 and H_2 transport properties of different **Pebax**® grades [71]: they prepared two polyether-polyamine films by melt extrusion, of thickness equal to 340 and 390 μm, having different content of the rigid PA segment (Nylon 12): 22 wt.% and 27 wt.% for Pebax®-2533 and Pebax®-3533, respectively. Permeation tests were carried out with a constant volume/variable pressure apparatus at temperatures up to 200 °C and with 10 bar feed pressure in single and mixed gas conditions. At 35 °C, the examined samples resulted CO_2-selective, with CO_2 permeability value of 350 and 230 Barrer for **Pebax®-2533** and **Pebax®-3533**, respectively, and ideal CO_2/CO selectivity values of ~ 16 for both samples. In the 35 to 100 °C temperature range, the activation energy for permeation in Pebax®-2533 was 6.5 kJ/mol for CO_2 and 19.4 kJ/mol for CO, confirming the

unfavorable effect of temperature on selectivity, that leads to a α value of about 8 at 100 °C.

Merkel *et al.* carried out a study on the transport of simulated syngas mixture (42 vol% H_2 − 46 vol% CO − 10.5 % CO_2 − 1.5 vol%H_2S) through a 100 μm thick **PTMSP** film supplied by Permea, Inc. (St Louis, MI) [93]. Test were carried out from room temperature to 240 °C, using a constant pressure/variable volume apparatus equipped with a gas chromatograph (GC). At $T = 23$ °C and $p_{feed} = 1.4$ bar a P_{CO} value of 5400 Barrer was found with ideal CO_2/CO selectivity ~ 3. Activation energy for CO_2 and CO permeation in the examined temperature interval for PTMSP was – 6.5 and – 2.1 kJ/mol, respectively. Consequently, the examined film samples exhibited lower CO_2/CO separation performances at higher temperature: at 150 °C the CO_2/CO selectivity was, in fact, ~ 2. Interestingly, in spite of its glassy nature, penetrant permeability in PTMSP was proved to follow a solubility-driven behavior, in a similar fashion to polymer rubbers: that has to be ascribed to the large free volume of the polymer. It was also noted that PTMSP exhibited accelerated physical aging at elevated temperatures [93].

Park *et al.* studied also **Pebax 1657** and **1074** membranes provided by Arkema Inc. (France) and measured CO_2 permeability values of 55.9 and 87.5 Barrer, respectively, with CO_2/CO selectivity values close to 30 at 25 °C and 2.7 bar feed pressure [94]. This selectivity value is larger than that of polyimides and suggest rubbery membranes with CO_2-philic PEO units exhibit better permeability and selectivity than glassy polyimide membranes, consistently with the solubility-controlled nature of this separation [76].

In a successive study, Park *et al.* reported on the CO_2/CO selective properties of CO_2- philic polymers prepared by free radical polymerization of **poly(ethylene glycol) methyl ether metacrylate** (PEGMA), methyl methacrylate (MMA) and 4-hydroxybenzophenone (BPMA) casted into thin precursor film and then crosslinked by UV-induced photochemical reaction [94]. The authors studied the gas transport properties of the rubbery membranes by pure gas permeation tests at 30 °C in a variable pressure/constant volume chamber. They observed that the CO_2 permeability increased with the content of the CO_2- philic PEGMA from 49.7 Barrer at 60 wt.% to 110.7 Barrer at 90 wt.%. This increase was correlated to: i) an improved CO_2 solubility due to the interaction between the PEGMA polar ether groups and the quadrupolar CO_2 molecule and ii) an increased CO_2 diffusivity ascribed to the larger polymer chain flexibility as suggested by the decrease of the T_g values. Changing the PEGMA content, no variation was observed on the CO_2/CO selectivity, ~ 30 [94].

In conclusion of this section on high permeability polymers (PDMS, Pebax, PTMSP), we can state that: *i*) Such polymers show high and ultra-high values of CO_2 permeability, ranging from 55 to 18,200 Barrer depending on the material, with the highest value shown by PTMSP; *ii*) the CO_2/CO selectivity is inversely correlated to the permeability, and has the lowest value (3.4) for PTMSP while reaches values of 30 for Pebax 1657 and 1074; *iii*) the activation energy for CO_2 permeation in these materials is very low and, in some cases, even negative: as a consequence, there is a rapid decay of selectivity with temperature.

3.4. Biopolymers

Polylactic acid (PLA) is derived from renewable resources, such as corn starch or sugarcanes, and it is currently the most widely studied biopolymer given its biodegradable and compostable nature for applications in the packaging field, in the medical device market and as a membrane material [95]. The CO_2/CO selective properties of dense, nearly amorphous PLA films were studied by Checchetto *et al.* using film samples prepared by solution casting method from PLA pellets provided by Nature Works (LLC, PLA 4032D) with chloroform as solvent. Tests were carried out in dead-end configuration analyzing the permeation of CO_2, CO, N_2 and O_2 in single and mixed gas conditions with feed pressure up to 1 bar at temperatures between 25 and 80 °C [70,96]. At 25 °C the PLA membrane exhibited CO_2 and CO single gas permeability values of 1.12 and 0.07 Barrer, respectively, and ideal CO_2/CO selectivity ~ 15. The CO_2 and CO diffusivity values were 4.0×10^{-9} and 9.4×10^{-9} cm^2/s, respectively. The CO_2/CO selectivity decreased with temperature: in single gas tests at 65 °C, in fact, the P_{CO_2} and P_{CO} values were 3.2 and 0.37 Barrer, respectively, and the CO_2/CO selectivity decreased to ~ 10. No remarkable variations of gas permeability and selectivity were observed exposing the membrane sample to ternary CO_2, CO, O_2 and quaternary CO_2, CO, N_2, O_2 gas mixtures as in the low-pressure interval considered competitive sorption effects and plasticization phenomena are negligible. Activation energy values for CO_2 permeation and diffusion were 22.4 and 39 kJ/mol, respectively while those for CO were 36 and 47 kJ/mol, respectively [70,96].

Cellulose Acetate is the most important cellulose ester and has biodegradable properties; it is produced in form of films used for photographic and packaging purposes owing to its transparency and low cost; its use is investigated for medical applications such as drug delivery systems and wound dressing and for membrane technology [97]. Feldman *et al.* prepared cellulose acetate films 18 to 30 μm thick by solution casting method using cellulose acetate provided by Aldrich Co. and tetrahydrofuran (THF) as solvent [98]. The authors obtained at 24 °C and 2.1 bar feed $P_{CO_2} = 8.5$ Barrer and $P_{CO} = 0.15$ Barrer, evidencing a remarkably high CO_2/CO selectivity of ~ 60. Increasing temperature to 50 °C, a sharp increase of the CO permeability to 0.5 Barrer was observed, without significant variations of the CO_2 transport rates, thus evidencing a decrease of the CO_2/CO selectivity value ~ 20. The authors observed that the addition of transition metal atoms (Ru) to the polymeric matrix produced a significant decrease of the CO_2 permeability, P_{CO_2} = 1.6 and 4.8 Barrer at 24 and 50 °C, respectively, without noticeable effects on the CO transport rates, thus worsening the CO_2/CO selectivity. The P_{CO2} value measured by Feldman is compatible with the value of 6.3 Barrer recently measured in single gas test at 25 °C and 10 bar feed pressure with films prepared by solution casting by Najafi *et al.* using glassy CA purchased by Eastman Co. (CA-398–30) and N,N-Dimethylformamide (DMF) as solvent [99], as well as the P_{CO} value obtained by McCandless with DuPont 100 CA-43 cellulose acetate film of 0.35 Barrer at 30 °C (increasing to 1.71 Barrer at 100 °C) [82].

Parylene is the common name of "green" polymers members of the xylylene family having backbone made of *para*-benzenedyil rings ($-C_6H_4-$) connected by 1,2-ethanedyil bridges ($-CH_2-CH_2-$)[79]. These linear polymers are classified as thermoplastic and are characterized by a polycrystalline structure. They are considered "green" polymers because their polymerization needs no initiator or other chemical to terminate the chain. Parylene coatings can be easily deposited by Chemical Vapor Deposition (*CVD*) in atmosphere of monomer *para*-xylylene $H_2C = C_6H_4 = CH_2$ and are employed as moisture barrier and protection against corrosion and in biomedical applications [100]. McCandless studied the CO and H_2 transport through Parylene C (polychloro-p-xylylene) and Parylene N (poly-p-xylylene) films provided by Union Carbide and at 30 °C found P_{CO} values of 0.013 and 0.11 Barrer, respectively [82]. Yeh *et al.* studied the gas transport properties of Parylene C and Parylene N films samples prepared by vacuum pyrolysis of cyclic p-xylylene [101]. Gas transport tests were carried out at 25 °C and 1 bar feed pressure. The authors found that gas transport through Parylene C films with 20 to 50 vol.% crystalline fraction exhibited P_{CO} value of 0.2 Barrer and D_{CO_2} value of $(2 \div 3) \times 10^{-9}$ cm^2/s, while Parylene N, with a lower crystalline fraction, 10 to 30 vol.%, has larger P_{CO2} values, ~ 2 Barrer, and similar D_{CO_2} values, $(2 \div 3) \times 10^{-8}$ cm^2/s. The scaling of the CO_2 transport rates between Parylene C and N is in line with the scaling of the CO permeability value observed by McCandless [82]. Comparing data reported by McCandless with data reported by Yeh, a CO_2/CO selectivity value of ~ 15 and ~ 18 can be estimated for Parylene C and Parylene N, respectively (see Table 3, 4, 5, 6, 7, 8, 9).

Table 3
Single gas permeability (P) and diffusivity (D) values of CO and CO_2 of the PI films prepared using BPDA and ODA. α: ideal selectivity, α_D: diffusivity selectivity, α_S: solubility-selectivity [72]. ρ: sample mass density.

Sample preparation	T (°C)	P_{CO2} Barrer	D_{CO2} cm^2/s	P_{CO} Barrer	D_{CO} cm^2/s	α	α_D	α_S
Dried at 170 °C, 20 h vacuum. ρ = 1.366 g/cm^3	50	0.715	2.53 × 10^{-9}	0.055	2.1 × 10^{-9}	13	1	13
Imidized at 230 °C, 10 h In vacuum. ρ = 1.375 g/cm^3	50	0.429	1.72 × 10^{-9}	0.032	–	13	–	–
Annealed at 290 °C, 3 h in N_2 flow. ρ = 1.403 g/cm^3	50	0.11	0.70 × 10^{-9}	0.008	–	13	–	–
Annealed at 300 °C, 2 h in N_2 flow. ρ = 1.409 g/cm^3	50	0.090	0.64 × 10^{-9}	0.007	–	13	–	–

3.5. Polyurethanes

Polyurethanes (PU) form a class of block copolymers where organic units are joined by urethane ($-NHCOO-$) groups and are obtained by poly-addition from three components: macro-diols, diisocyanates and cross-linkers. Given the large number of monomers available for their production, a large variety of PU can be synthesized with tunable properties, for applications as rigid or flexible foams, fibers, adhesives and coatings [102]. Pecoraro *et al.* carried out a series of systematic studies on the gas transport properties of PU films prepared with **TDI** (a 2,4 and 2,6 toluene diisocyanate $CH_3-C_6H_3(NCO)_2$ mixture in 80/20 ratio) and different polymeric diols with the aim of preparing amorphous PU films with different chemical nature, able to modulate the gas transport properties. PU film samples were prepared using TIPA (triisopropanol amine $N-[CH_2CH-(CH_3)OH]_2$) as cross-linking agent and dehydrated ethyl acetate as solvent. In a first study, the authors prepared PU containing polypropylene glycol (PPG) or polyester groups (poly tetramethylene glycol PTMA) with different molecular weights [103]. In a successive study, the authors prepared PU films using TDI and polymeric diols containing polar groups, specifically polycarbonate diols, poly ether carbonate diols, poly ester carbonate and polyester diols [104]. Gas transport tests were carried out at 1 bar feed pressure and T = 35 °C using polymer films with thickness of about 100 μm. Relevant information on the transport properties of the PU films are reported in Table 10. The authors found that increasing the molecular weight of the diol there was a decrease of the glass transition temperature (T_g) value of the PU sample accompanied by an increase of the CO_2 and CO diffusivities and permeabilities. A plot of the CO_2 and CO permeability and diffusivity values as function of the T_g value is reported in Fig. 3. The decrease of diffusivity (and permeability) with polymer T_g is often observed for rubbery polymers, as such parameters provide an indication of polymer segmental mobility, and the ease of creating free volume pockets in the macromolecular matrix. The lower the T_g (with respect to measurement temperature, i.e. room T in this case), the larger the chain mobility, and the higher the diffusion coefficient. Analogous correlation can be found for permeability, since the glass transition temperature has a very limited effect on solubility.

Using the poly (hexamethylene carbonate) diol (PEMC), for example, increasing its weight average molecular weight (M_W) value from 565 to 2370, the T_g value of the PU sample decreased from 38.5 to − 20 °C and

Table 4
Single gas permeability (P) and diffusivity (D) values of CO and CO_2 of the PI films prepared using BPDA and ODA, MDA, DDS and DDBT and of fluorinated and non-fluorinated PI films and of PI films prepared using 6FDA anhydride and methyl substituted phenilenediamines [73–75]. α: ideal selectivity, α_D: diffusivity selectivity, α_S: solubility-selectivity.

polyimide	T (°C)	P_{CO2} Barrer	D_{CO2} cm^2/s	P_{CO} Barrer	D_{CO} cm^2/s	α	α_D	α_S
BPDA-ODA	50	0.87	2.65 × 10^{-9}	0.066	2.10 × 10^{-9}	13.2	1.3	10
BPDA-MDA	50	2.17	5.5 × 10^{-9}	0.16	3.9 × 10^{-9}	13.6	1.4	9.7
BPDA-DDS	50	2.57	4.7 × 10^{-9}	0.186	3.02 × 10^{-9}	13.8	1.6	8.6
BPDA-DDBT	50	8.2	8.3 × 10^{-9}	0.47	4.2 × 10^{-9}	17.4	1.9	9.2
PMDA-mp'ODA	35	1.18	0.28 × 10^{-8}	0.087	0.14 × 10^{-8}	13.6	2	6.8
PMDA-pp'ODA	35	3.55	0.80 × 10^{-8}	0.270	0.4 × 10^{-8}	13.1	1.9	6.9
PMDA-BAPHF	35	17.6	4.1 × 10^{-8}	1.48	2.4 × 10^{-8}	11.2	1.7	6.6
PMDA-BATPHF	35	24.6	5.3 × 10^{-8}	2.10	2.7 × 10^{-8}	11.7	1.9	6.2
BPDA-pp'ODA	35	0.642	0.18 × 10^{-8}	0.036	–	17.8	–	–
BPDA-BAPHF	35	4.96	1.4 × 10^{-8}	0.405	0.59 × 10^{-8}	12.1	2.4	5.0
BPDA-BATPHF	35	9.15	2.4 × 10^{-8}	0.768	1.1 × 10^{-8}	11.9	2.2	5.4
BPDA-BAHF	35	27.7	4.6 × 10^{-8}	2.16	2.3 × 10^{-8}	12.8	2	6.4
BTDA-pp'ODA	35	0.625	0.19 × 10^{-8}	0.05	0.11 × 10^{-8}	12.5	1.7	7.4
BTDA-BATHF	35	4.37	1.2 × 10^{-8}	0.313	0.58 × 10^{-8}	14.0	2.1	6.7
BTDA-BATPHF	35	6.94	1.8 × 10^{-8}	0.549	0.76 × 10^{-8}	12.6	2.4	5.3
BTDA-BAHF	35	10.1	1.7 × 10^{-8}	0.699	0.58 × 10^{-8}	14.4	2.9	5.0
6FDA-mp'ODA	35	6.11	1.4 × 10^{-8}	0.414	0.55 × 10^{-8}	14.8	2.5	5.9
6FDA-APAP	35	10.7	2.2 × 10^{-8}	0.776	0.93 × 10^{-8}	13.8	2.4	5.8
6FDA-pp'ODA	35	16.7	3.1 × 10^{-8}	1.16	1.4 × 10^{-8}	14.4	2.2	6.5
6FDA-BAPHF	35	19.1	4.2 × 10^{-8}	1.51	2.3 × 10^{-8}	12.6	1.8	7.0
6FDA-BATPHF	35	22.8	5.7 × 10^{-8}	1.82	1.9 × 10^{-8}	12.5	3	6.2
6FDA-BAHF	35	51.2	8.1 × 10^{-8}	4.14	3.4 × 10^{-8}	12.4	2.4	5.2
6FDA-mPD	35	9.2	1.7 × 10^{-8}	0.71	7.50 × 10^{-9}	12.9	2.3	5.6
6FDA-mMPD	35	40.1	6.2 × 10^{-8}	3.14	2.50 × 10^{-8}	12.8	2.5	5.1
6FDA-mTrMPD	35	431	54 × 10^{-8}	48.3	3.20 × 10^{-7}	8.9	1.7	5.2
6FDA-pPD	35	15.3	2.6 × 10^{-8}	1.15	1.20 × 10^{-8}	13.3	2.2	6

(*continued on next page*)

Table 4 (*continued*)

polyimide	T (°C)	P_{CO2} Barrer	D_{CO2} cm^2/s	P_{CO} Barrer	D_{CO} cm^2/s	α	α_D	α_S
6FDA-pDiMPD	35	42.7	6.5×10^{-8}	3.71	2.80×10^{-8}	11.5	2.3	5
6FDA-pTeMPD	35	440	48×10^{-8}	51.9	3.20×10^{-7}	8.5	1.5	5.7
6FDA-mTrMPD	35	137	16.4×10^{-8}	13	8.18×10^{-8}	10.5	2	5.2

Table 5
Single gas permeability (P) and ideal selectivity (α) of semi-alicyclic aromatic polyimides films [76].

Polyimide	T (°C)	P_{CO2} (Barrer)	P_{CO} (Barrer)	α
DOCDA-pDPDA	25	8.60	0.662	13.0
DOCDA-BAPF	25	8.60	0.610	14.1
DOCDA-MDA	25	3.13	0.170	18.4
DOCDA-ODA	25	1.71	0.110	15.5
DOCDA-pPDA	25	0.74	0.090	8.2

the P_{CO_2} and P_{CO} values increased from 1.4 and 0.06 Barrer, respectively, to 15 and 1 Barrer, respectively. The increase of the gas transport rates with the diol M_W was accompanied by a CO_2/CO selectivity reduction from ~ 23 for the PU sample with $T_g = 38.5$ °C to ~ 15 for the one with $T_g = -20$ °C. Diffusivity values for the two penetrants were nearly equivalent: the D_{CO_2}/D_{CO} ratio was, in fact, ~ 1.5.

To summarize: *i*) the CO_2 permeability of polyurethanes varies between 0.7 and 72 Barrer, depending on the chemical composition, and it increases with the molecular weight of the polyester groups;

ii) the CO_2/CO selectivity lies in a narrow range, between 5.6 and 24.6, with a decreasing trend on the molecular weight, and *iii*) the diffusivity-selectivity varies between 0.7 and 2.6.

3.6. Other thermoplastic polymers

Fluoropolymers exhibit exceptionally high chemical stability, low surface energy, low friction coefficient and high-water repellency thanks to the strong $C-F$ polar bond. Commercial fluoropolymers are polyvinyl fluoride (PVF), polytetrafluoroethylene (PTFE) and polyvinylidene fluoride (PVDF) [105]. Polyvinyl fluoride (PVF) is the homopolymer of vinyl fluoride and is commercialized by Chemours™ in form of biaxially oriented films with the name **Tedlar**®. McCandless measured the *CO* and H_2 permeability values of Tedlar® films in cross flow configuration with 3.5 bar feed pressure and obtained at 30 °C a P_{CO} value of 0.009 Barrer and a P_{H_2} value of 0.6 Barrer [82]. Mohr and Paul measured a H_2 permeability value (0.54 Barrer at 35 °C) in line with those reported by McCandless, while a 0.27 Barrer was obtained for CO_2 [106]. Values measured by the producer via the ASTM D-1434 Test Method were somewhat lower than those coming from the two other sources, being 0.35 Barrer for H_2 and 0.067 Barrer for CO_2 at 24 °C [107].

Styrene is used as a monomer to prepare different plastic materials such as **polystyrene** (PS), **acrylonitrile–butadiene–styrene copolymer** (ABS) and **styrene-acrylonitrile** (SAN). PS is glassy at room temperature and has limited limited flexibility [87,108]. McCandless studied the *CO* permeation through PS films without reporting information on the membrane sample supplier and obtained at 30 °C a P_{CO} value of 0.92 Barrer [82]. CO_2 permeability values of PS films were provided in technical reports of different suppliers: at 25 °C a P_{CO_2} value of 6.0 to 8.9 Barrer is reported for Styron™ PS [109], a value of 8.0 Barrer for INEOS Styrolution AG Polystyrol 168 N GPPS Film [110] and value between 4.2 and 6.6 Barrer for Dow Chemical Trycite™ Oriented PS Film [111]. The P_{CO} value of 0.92 Barrer reported by McCandless at 30 °C suggests that PS is poorly CO_2-selective exhibiting a CO_2/CO selectivity value ~ 5.

Polyesters are polymers containing ester functional group in every repeating unit of their main chain. Commercial polyesters include bisphenol-A polycarbonate (PC), a good electrical insulator exhibiting heat resistant and flame-resistant properties mostly used for electronic application, polyethylene terephthalate (PET), widely used in fibers for clothing and to produce containers for liquids and food, as well as polybutylene terephthalate (PBT), often employed as insulator in the electrical and electronic industry [112]. Mylar® is the brand name of DuPont commercial biaxially-oriented **PET** (crystalline fraction ~ 36 %) [113]: McCandless measured the *CO* permeability of Mylar type S films and obtained the value of 0.019 Barrer at 30 °C and of 0.17 Barrer at 100 °C [82], while a CO_2 permeability value at 25 °C of 9.7×10^{-2} Barrer is reported in the technical sheet, indicating that Mylar exhibits poor CO_2 selective properties with CO_2/CO selectivity values ~ 5. Note that Lewis *et al.* found at 25 °C CO_2 permeability values of 0.37 Barrer

Table 7
Single gas permeability (P) and ideal selectivity (α) of high permeability polymers. [*]: values mentioned as ref. 11 in ref. [92].

Polymer	T (°C)	P_{CO2} (Barrer)	P_{CO} (Barrer)	α
PDMS [92]	35	3700	440	8.4
PDMS [93]	23	3200	500	6.4
PDMS [*]	–	2700	300	9
Pebax 2533 [92]	35	350	21.9	16
Pebax 3533 [92]	35	230	14.4	16
Pebax 1657 [76]	25	55.9	1.9	30
Pebax 1074 [76]	25	87.5	2.9	30
PTMSP [93]	23	18,200	5400	3.4

Table 8
Single gas CO_2 and *CO* permeability (P), CO_2 diffusivity (D) and ideal CO_2/CO selectivity (α) of cross-linked poly(PEGMA-co-MMA-co-BPMA) membranes with different PEGMA content (*CO* diffusivity data are not reported) [94].

PEGMA content	T (°C)	P_{CO2} (Barrer)	D_{CO2} (cm^2/s)	P_{CO} (Barrer)	α
90 wt%	30	110.7	0.54×10^{-8}	3.68	30 ± 1
80 wt%	30	77.3	0.44×10^{-8}	2.64	29 ± 1
70 wt%	30	69.9	0.41×10^{-8}	2.37	29 ± 1
60 wt%	30	49.7	0.33×10^{-8}	1.92	26 ± 2

Table 6
Permeability (P) and diffusivity (D) of commercial polyimide films. α: ideal selectivity, α_D: diffusivity selectivity, α_S: solubility-selectivity.

Polyimide	T (°C)	P_{CO2} (Barrer)	D_{CO2} (cm^2/s)	P_{CO} (Barrer)	D_{CO} (cm^2/s)	α	α_D	α_S
Upilex® [72]	50	0.16	8.4×10^{-10}	0.01	7×10^{-10}	13.3	1.2	11.1
Matrimid® [80]	25	8.1	2.2×10^{-9}	0.5	3.9×10^{-9}	16.2	0.6	28.7
Matrimid® [81]	30	6.4	–	0.45	–	14.2	–	–
Kapton® [83]	50	0.51	–	0.02	–	22.2	–	–
Ultem® [85]	25	0.3	1×10^{-8}	0.05	0.6×10^{-8}	6	1.5	4
PEI [80]	25	1.17	8.5×10^{-9}	0.07	1.1×10^{-8}	16	0.8	20

Table 9
Single gas CO_2 and CO permeability (P), diffusivity (D) and ideal selectivity (α) of biopolymers at different temperatures. Selectivity values for Parylene C and N were obtained using ref. 101 for CO_2 and ref. 82 for CO.

Polymer	T (°C)	P_{CO2} (Barrer)	D_{CO2} (cm^2/s)	P_{CO} (Barrer)	D_{CO} (cm^2/s)	α	α_D	α_S
PLA [80,96]	25	1.12	4.0×10^{-9}	0.07	9.4×10^{-9}	16	0.43	37
CA [98]	24	8.5	–	0.15	–	5713		
	50	9.8	–	0.5	–			
CA [99]	25	6.5	–		–	–		
CA [82]	30	–	–	0.35	–	–		
	100	–	–	1.71	–	–		
Parylene C [82]	30	–	–	0.013	–	–		
Parylene N [82]	30	–	–	0.11	–	–		
Parylene C [101]	25	0.2	$(0.2 \div 0.3) \times 10^{-8}$	–	–	15		
Parylene N 101]	25	2	$(2 \div 3) \times 10^{-8}$	–	–	18		

Table 10
Single gas permeability (P) and diffusivity (D) values of the polyurethane films as measured at 1 atm feed pressure. α: ideal selectivity, α_D: diffusivity selectivity, α_S: solubility-selectivity [103,104]. List of used diols: poly (oxypropylene) glicols: VR: Voranol. Polycarbonate diols: PTMC: poly(trimethylene carbonate); PEMC: poly (hexamethylene carbonate); PPMEMC: poly(pentamethylene-hexamethylene carbonate). Polyethercarbonate diols: PTEGC: poly(triethylene glycol carbonate) diol; PDPGC: poly(dipropylene glycol carbonate) diol.; PDPGPPGC: poly(dipropylene glycol)poly(propylene glycol) diol. Polyestercarbonate diols: P(C-ES): poly(hexamethylene carbonate pentamethylene ester) polyester diols: PTMA: poly(tetramethylene adipate).

Polymer	T (°C)	P_{CO2} Barrer	D_{CO2} (cm^2/s)	P_{CO} Barrer	D_{CO} (cm^2/s)	α	α_D	α_S
VR 400-PU	35	0.95	2.8×10^{-8}	0.05	2.0×10^{-9}	19	1.4	13.6
VR 1200-PU	35	19.0	23×10^{-8}	3.4	28×10^{-9}	5.6	0.8	7
VR 2000-PU	35	72	15×10^{-7}	9.2	58×10^{-9}	7.8	2.6	3
PEMC 565-PU	35	1.4	2.2×10^{-8}	0.06	1.5×10^{-9}	23.3	1.5	15.9
PEMC 840-PU	35	2.7	2.9×10^{-8}	0.2	3.9×10^{-9}	13.5	0.7	19.3
PEMC 1025-PU	35	3.8	3.8×10^{-8}	0.3	5.6×10^{-8}	12.7	0.68	18.7
PEMC 1900-PU	35	15	21×10^{-8}	1.0	14×10^{-8}	15.0	1.5	10
PTMC 670-PU	35	0.9	1.2×10^{-8}	0.07	1.0×10^{-8}	12.9	1.2	10.8
PTMC 1093-PU	35	1.8	1.7×10^{-8}	0.14	3.3×10^{-8}	12.9	0.5	25.8
PPMEMC 1700-PU	35	10	8.9×10^{-8}	0.59	7.4×10^{-8}	16.9	1.2	14.1
PTEGC 2100-PU	35	4.2	5.0×10^{-8}	0.19	6.3×10^{-8}	22	0.8	27.5
PDPGC 2537-PU	35	3.6	3.5×10^{-8}	0.18	3.3×10^{-8}	20	1.1	18.2
PDPGPPGC 1545-PU	35	9.7	6.1×10^{-8}	0.78	16×10^{-8}	12.4	0.4	31
PC-ES 2000-PU	35	27.0	16×10^{-8}	1.00	24×10^{-8}	27	0.7	38.6
PTMA 600-PU	35	0.7	2.7×10^{-8}	0.04	3.9×10^{-8}	18.9	0.7	27
PTMA 1000-PU	35	6.4	5.7×10^{-8}	0.26	7.4×10^{-8}	24.6	0.8	32
PTMA 1600-PU	35	20	13×10^{-8}	1.2	11×10^{-8}	16.7	1.2	13.9

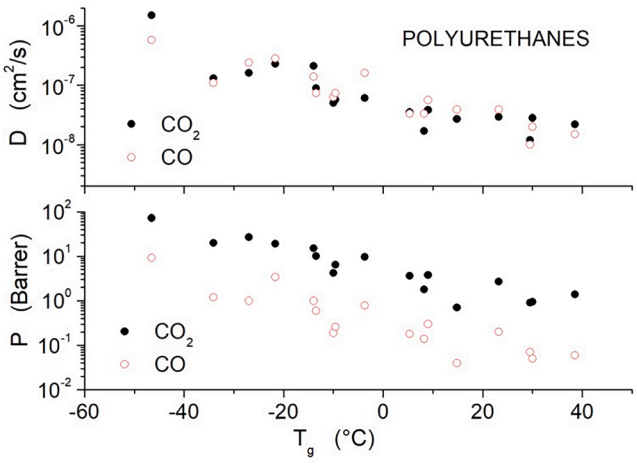

Fig. 3. Permeability and diffusivity of CO_2 and CO in the polyurethane series as function of polymer glass transition temperature T_g [103,104].

for amorphous films [114], while Mapes *et al.* found a P_{CO_2} value of 0.49 Barrer at 22 °C for 44 μm thick Mylar vacuum windows [115].

Polysulfones (PSF) are high performance amorphous glassy polymers which contain an aryl-SO_2-aryl subunit responsible of their toughness and stability at high temperature. PSF are chemically inert, hydrolytically, thermally and oxidatively stable and highly biocompatible but, given the high production costs, are generally used in specialty applications such as the construction of appliance parts exposed to high temperature or corrosive media, automotive/aerospace and applications [116]. Functionalized polysulfones are used as membrane materials for different processes such as water filtration, recovery of biofuels via pervaporation and gas (CO_2/CH_4) separation [117]. The gas transport properties of amorphous PSF films prepared by solution-casting were studied by different authors: McHattie *et al.* [118] obtained at 35 °C with 1 atm CO_2 feed pressure a P_{CO_2} value of 5.6 Barrer and a D_{CO_2} value of 2 $\times 10^{-8}$ cm^2/s, equal to the value of 5.61 Barrer found by Nasarian *et al.* at 30° C and 10 bar feed pressure [~~98~~ [119] and compatible with the values of 4.9 Barrer reported by Robeson at 35° C [59], of 5.4 Barrer reported by Scholes *et al.* (35° C and feed pressure between 6 and 14 bar [120]) and the value of 6.5 Barrer reported by Ahn *et al.* (35 °C with 4.4 barm CO_2 transmembrane pressure, with D_{CO_2} value of 1.2×10^{-8} cm^2/s) [121]. McCandless studied the CO transport through a Sulfone 47 film produced by Union Carbide and obtained a P_{CO} value of 0.37 Barrer at 30 °C and of 1.2 Barrer at 100 °C [82]. Considering the P_{CO} value of 0.37 Barrer obtained by McCandless, it can be readily concluded that PSF membrane are CO_2 selective and that CO_2/CO selectivity values no worse than ~ 13 can be expected.

Polyamides (PA) are semi-crystalline polymers typically produced by the condensation of a diacid and a diamine; high-molecular weight polyamides are commonly known as Nylon [122]. Caprolactam is a ring-structured organic molecule with six C atoms having chemical formula

$(CH_2)_5C(O)NH$ used to produce Nylon 6 [123]. McCandless obtained at 30 °C a P_{CO} value ~ 0.01 Barrer studying polycaprolactam films provided by Allied Chemical and Dye Co. [82]. The gas transport properties of Nylon 6 films were studied by Guisheng *et al.* using CO_2/O_2 /N_2 mixtures, who found at 30 °C a P_{CO_2} of 0.19 Barrer [124]. Comparing the two sets of data, it can be concluded that Nylon 6 films are CO_2 selective offering good CO_2/CO selectivity ~ 19, unfortunately accompanied by low CO_2 transport rates.

Sakaguchi *et al.* carried out systematic studies on the *CO* transport through separation membranes made of aromatic polyamide containing sulfone linkages in the main chain: they prepared film samples consisting of bis[4-(4-aminophenoxy)phenyl]sulfone (**4SED**), *m*-phenylenediamine (**MPD**) and *iso*-phthaloyl dichloride (**ICP**) [125] and observed *CO* permeability value at 30 °C decreasing from ~ 0.1 Barrer for the sample containing 100 % 4SED diamine to about 0.03 Barrer for samples containing mixed diamines at 30 % 4SED and 70 % MPD diamine ratio. This permeability decrease was due to restricted *CO* mobility because the measured D_{CO} value decreased from 1.8×10^{-9} to 5.6×10^{-10} cm^2/s. In a successive study, the authors prepared copolymer synthesized from ICP and mixed diamines consisting on various ratios of bi(3-aminophenil) sulfone (3DDS) and *m*-phenylenediamine (MPD) [126] and measured the permeability values for H_2 and *CO* at 30 °C in single gas conditions (the feed pressure value was not reported). The permeability value for *CO* of the poly(sulfone-diamine) sample containing 3DDS was 0.01 Barrer with *CO* diffusivity value ~ 7×10^{-10} cm^2/s ($P_{H_2}/P_{CO} = 150$); when the mixed diamine contained 30 % a small ~ decrease for P_{CO} was reported accompanied by a similar decrease of the *CO* diffusivity value and $P_{H_2}/P_{CO} = 185$. The authors also observed that solvent removal by the thermal treatment of the as-cast membrane in the 50 to 200 °C interval progressively reduced the P_{CO} value and increased the H_2/CO selectivity, as a result of the densification of the membrane as suggested by the observed reduction of the *CO* diffusivity values [127].

In general, the materials inspected in this paragraph (fluoropolymers, polyesters, polyamides), show very low values of permeability and/or selectivity for the CO_2/CO separation. Data are very scattered and there is a lack of systematic experimental data to examine the CO_2/CO properties. Some important polymers used in membrane separations, e.g., amorphous Teflons, are completely missing from this characterization, as the permeability of CO was never assessed. One of the most notable performances is that of polysulfone, showing a CO_2 permeability value of 5.6 Barrer and an estimated selectivity of 15.

3.7. *Effects of **CO** contaminants in the feed mixture on the **CO_2** transport properties*

Few studies are present in literature evidencing the effect of *CO* impurities on the operative performances of membranes exposed to gas mixtures. Scholes *et al.* studied the CO_2 transport through ~ 40 μm thick flat dense Matrimid® membranes prepared by solution casting using as a feed gas a binary CO_2/N_2 gas mixture containing H_2S and *CO* impurities. Tests were carried out at $T = 35$ °C with a constant volume, variable pressure gas permeation apparatus in cross-flow configuration with the permeate side of the membrane kept at atmospheric pressure [128]. It was observed that the presence of *CO* reduced the CO_2 permeability from 5.1 Barrer to 4.5 Barrer when the *CO* partial pressure increased from 0 to 1 kPa: the authors attributed this effect to competitive CO_2 – *CO* sorption effects. No test was carried out to evaluate the *CO* transport parameters. The authors also studied the permeation of unshifted syngas mixture (16.2 mol.% CO_2, 9.8 mol.% H_2, 63.2 mol.% N_2, 6.7 mol.% *CO*, 2.8 mol.% CH_4, 0.25 mol.% H_2O and H_2S traces) through an asymmetric Matrimid® membrane, and observed a ~ 60 % decrease of the CO_2 permeance with respect to the value obtained with the CO_2/N_2 mixture, to be attributed to competitive CO_2 sorption effects with *CO* and H_2. The authors evaluated a CO_2/CO selectivity of 3.3 at 35 °C for the asymmetric Matrimid® membrane with the unshifted syngas. A reduction of the CO_2 permeability of 10 % compared to value obtained in single gas test at 600 kPa was observed by the same authors studying the gas transport through flat dense polysulfone and 6FDA-TMPDA membrane samples when the feed gas mixture contained 1000 ppm *CO* [120]. Similar effects of *CO* in gas mixtures were reported by Chen *et al.*, who observed that the CO_2 permeability of membranes fabricated by modifying a polymer-silica hybrid matrix (PSHM) with poly(ethylene glycol) dimethyl ether (PEGDME) was reduced by ~ 8 % by introduction of *CO* in the feed stream: no effort was done to evaluate the *CO* transport properties of the examined membrane [129].

4. Performance plot and upper bound

The ideal CO_2/CO selectivity as a function of the P_{CO2} value for the previously discussed membrane samples are reported in Fig. 4 (Robeson's plot). The upper-left panel is pertinent to the polyimide (PI) membrane samples while the upper-right one to the polyurethane membrane samples. The lower-right panel reports P_{CO_2}/P_{CO} selectivity data obtained with polyethylene and High Free Volume membrane samples, while selectivity data pertinent to other membrane samples are reported in the lower-left panel. The dashed horizontal lines in each figure mark the $P_{CO_2}/P_{CO} = 7$ and the $P_{CO_2}/P_{CO} = 20$ selectivity lines: these lines are reported as the P_{CO_2}/P_{CO} selectivity values of most reported membrane samples lie between them. The solid line in each figure describes the Robeson upper bound determined in a purely empirical fashion, similarly to the original reference [57]:

$$P(Barrer) = 1.1543 \times 10^{9} \cdot \alpha^{-4.7619} \quad (13)$$

This line has the same slope, but is shifted upwards, with respect to the one that we reported in our previous paper which was, $P(Barrer) = 1.7762 \times 10^{8} \cdot \alpha^{-4.7619}$ (see dotted line in each figure), which was calculated using a smaller set of polymer membrane data [80].

Looking at data illustrated in Fig. 4, we can recognize that at near room temperature conditions, only a small fraction of polymeric materials exhibit ideal selectivity values equal or higher than 20, and that only few of them lie above the proposed upper bound. Among the commercial polymers, **PVC**, **Kapton®** and **Parylene N** exhibit ideal selectivity ~ 20, **Matrimid®** ~ 16, but only the latter one exhibits acceptable CO_2 permeability values of 6.4 to 8.1 Barrer, although its performances are still positioned below the Robeson upper bound. All polyimides, whose separation behavior is usually governed by a size-selective mechanism, fall significantly below the upper bound line. **CA**, on the other hand, exhibits better separation properties than Matrimid®: at 24 °C its selectivity value is 60 withP_{CO_2} = 8.5 Barrer [98]. (see Table 11).

It also interesting to note that commercial semi-crystalline polymers exhibit P_{CO_2}/P_{CO} well below those suggested by the upper bound: **Grex** with 0.77 crystalline fraction, **Mylar®** with 36 % crystalline fraction and **Tedlar®** with 38 % crystalline fraction exhibit CO_2/CO selectivity of 1.9, 5 and 7, respectively, and P_{CO_2} lower than 1 Barrer. Such feature can be explained by the fact the crystallites do not actively participate to the transport process, thus lowering the permeability of the two key penetrants, with no improvement in the selectivity.

Among the polyurethane films, the light (1.17 g/cm^3) and rubbery (T_g = −27 °C) **PC-ES 2000 PU** exhibits good CO_2/CO separation properties, with ideal selectivity ~ 27 and P_{CO_2} values of 27 Barrer. The CO_2- philic **Pebax®** polymers exhibits the best separation properties, which are very close to the upper bound. **Pebax®-1657** (60 wt.% PEO – 40 wt.% PA6) and **Pebax®-1074** (55 wt% PEO – 45 wt% PA12) have P_{CO_2} = 55.9 and 87.5 Barrer, respectively, and ideal selectivity values close to 30. Reported data suggest that increasing the content of the CO_2-philic PEO blocks in **Pebax®** improves the P_{CO_2} values, to 350 Barrer in **Pebax®-2533** (80 wt% PEO – 20 wt% PA12) and 230 Barrer in **Pebax®-3533** (75 wt.% PTMO – 25 wt.% PA12), although reducing the polymer CO_2 selectivity to values ~ 16 [88]. **PEGMA-MMA-BPMA** samples at ~

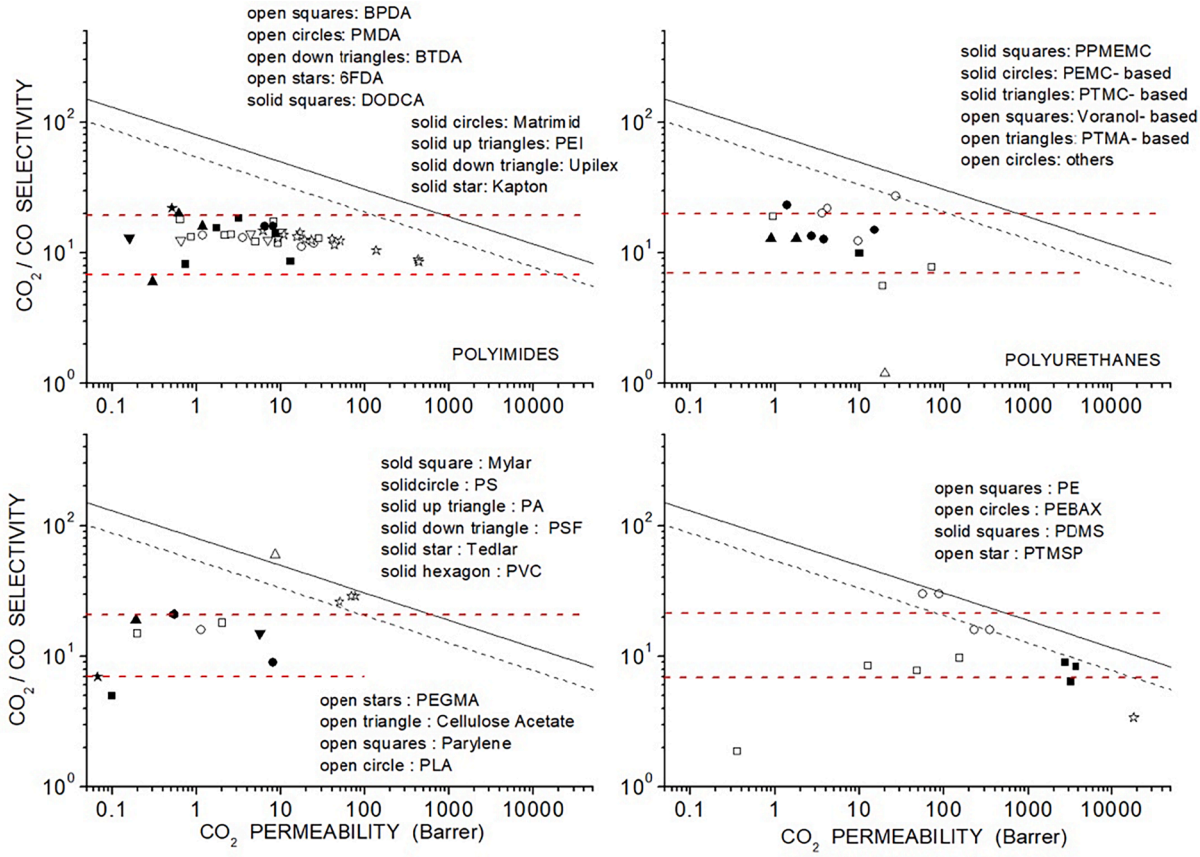

Fig. 4. CO_2/CO ideal selectivity (α) of the discussed polymeric films. (upper left). Polyimides [72–76,80,81,83,85]. (upper right). Polyurethanes [104,104]. (lower left). Green polymers [80,82,96,98,100], PEGMA-co-MMa-co-BPMA [76], Polyester. Mylar [82,113], polystyrene [82,110], PSF [61, 97, 98 82,118,119], PVF [82,107], PVC [65–69]. (lower right). polyethylene [62] and High Free Volume polymers [76,92,93]. The solid lines in all figures mark the upper bound defined by eq. (13) while the dotted lines are the upper bound as reported in [80]. The dashed horizontal lines mark the α = 7 and α = 20 values. (For interpretation of the references to color in this figure legend, the reader is referred to the web version of this article.)

Table 11
Single gas CO_2 and CO permeability (P), diffusivity (D) and ideal selectivity (α) of commercial polymers at different temperatures. [*]: technical sheet. Selectivity values for PS were always obtained ref. [82] for CO. Selectivity value for PET Mylar® was obtained using the Mylar® data sheet for CO_2 and ref. [82] for CO. Selectivity value for PSF was obtained using the Mylar technical sheet data for CO_2 and ref. [82] for CO.

Polymer	T (°C)	P_{CO2} (Barrer)	P_{CO} (Barrer)	α
PVF Tedlar® [82]	30		0.009	
PVF Tedlar® [107]	24	0.067	–	7
PVF Tedlar® [106]	35	0.27		30
PS [82]	30	–	0.92	–
PS Styron® [110]	25	6.0–8.9	–	6 ÷ 10
PS GPPS Ineos [110]	25	8.0	–	9
PS Oriented Dow [111]	25	4.2–6.6	–	5 ÷ 7
PET Mylar® S [82]	30	–	0.019	–
	100	–	0.17	
PET Mylar® [*]	25	0.097	–	5
PET amorphous [114]	25	0.37	–	–
PET Mylar [115]	22	0.49	–	–
PSF [118]	35	5.6	–	–
PSF [82]	30	–	0.37	15.1
	100	–	1.2	
Nylon 6 [82,124]	30	0.19	0.01	19

30 °C have ideal selectivity close to 30 and P_{CO_2} values increasing from 49.7 to 110.7 Barrer increasing the CO_2- philic PEGMA content from 60 to 90 wt%.

4.1. Empirical correlations

When looking at Robeson's papers [57], it can be noticed that for certain gas mixtures the tradeoff is more pronounced, i.e. varying the permeability has a strong inverse effect on the selectivity, which can span over orders of magnitude [57]. This is for instance the case of gases that differ markedly in molecular size such as He and CH_4; on the other hand, the O_2/N_2 or the He/H_2 separations show lower values of the slope representing the tradeoff mechanism, because of their similar molecular dimensions. Therefore, for such mixtures the size-selectivity of the polymers does not play a crucial role and so the tradeoff associated to it. Therefore, an increase of the free volume of the polymer will enhance the permeability to a similar extent for both gases and not affect significantly the selectivity.

As discussed in Section 2, the perm-selectivity of polymeric membranes to a generic gas couple α_{ij} has diffusive- selective character when the $\alpha_{ij}^D = \left(\frac{D_i}{D_j}\right)$ term dominates over the $\alpha_{ij}^S = \left(\frac{S_i}{S_j}\right)$ term, while it has solubility- selective character otherwise. Let us discuss the CO_2/CO selective properties of the reported membrane samples considering the experimentally obtained permeability and diffusivity values for the two penetrants reviewed in Section 3. This discussion will be carried out in the framework of the Freeman's model for the permeability/selectivity tradeoff in polymeric membranes [57–59].

The experimental D_{CO_2} and D_{CO} data for the different polymeric membranes are plotted in Fig. 5: each symbol reports in a log–log graph the measured CO diffusivity values (D_{CO}) in the y- scale vs. the measured CO_2 diffusivity value (D_{CO_2}) in the x- scale and is pertinent to a specific polymer. The D_{CO_2} as well as the D_{CO} values were measured at near

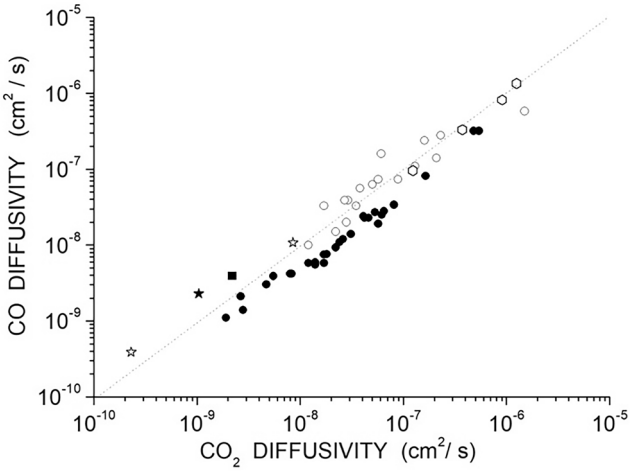

Fig. 5. Experimental D_{CO} vs D_{CO2} data measured at near ambient temperature in different polymers. Open circles correspond to polyurethane film samples [103,104], solid circles to polyimide films samples [73–75], open squares to polyetherimide film samples [80,85], solid square to PVC film sample [65,69], solid star to Matrimid® [80], open hexagons to polyethylene film samples [62].

ambient temperature by the same research team, thus by the same procedure and experimental set-up. The dashed line in Fig. 5 graphs the $\frac{D_{CO}}{D_{CO_2}} = 1$ equation. It can be observed that all experimental symbols lie close to this line, indicating that the CO_2 and CO diffusivity values, in the examined polymeric membranes, are comparable. In fact, a linear fit of the experimental data pertinent to the polyimide membranes provides the relation $\frac{D_{CO}}{D_{CO_2}} = 0.63 \pm 0.01$, while the fit of data pertinent to the polyurethane membranes $\frac{D_{CO}}{D_{CO_2}} = 1.00 \pm 0.15$.

The diffusion of a small molecule of *i*- specie in polymers is a thermally activated process, and a correlation was empirically observed between the pre-exponential factor D_{oi} and the activation energy for diffusion E_{Di}:

$$lnD_{0i} = a\frac{E_{Di}}{RT} - b \tag{14}$$

where the parameters a and c are independent on the nature of the penetrant molecule [130,131], evidencing that the activation entropy in the molecular jump is proportional to the activation energy [132]. According to the free volume theory of diffusion, this relation can be explained observing that in its migration through the polymeric layers, the penetrant molecule jumps to a neighbor free volume element having size large enough to accommodate it: the larger is the size of the hole, the higher is the energy E_{Di} needed to create it and the larger is the entropy change associated with its formation [133]. It was empirically observed that the parameter a is independent also on the polymer kind and exhibits the universal value of 0.64 [134] while the value of the parameter b is $-ln(10^{-4}cm^2/s) = 9.2$ in rubbery polymers and $-ln(10^{-5}cm^2/s) = 11.5$ in glassy polymers [56].

The activation energy for diffusion E_{Di} depends on the square of the penetrant molecule size d_i and the following relationship was empirically observed

$$E_{Di} = cd_i^2 - f \tag{15}$$

where c and f are polymer-dependent parameters: this finding was explained by Meares considering that the activation energy is proportional to the volume of the FVE where the molecule jumps, which is given by the product of the penetrant diameter squared and the jump length [135]. Van Krevelen reported values for c ranging from 250 cal/(mol Å)^2 for flexible polymers to 1100 cal/(mol Å)^2 for stiff-chain polymers and f values ranging from 0 to 12000 cal/mol for rubbery polymers and polyimides, respectively [56]. Eq. (10) suggests that polymers having high diffusivity selectivity necessarily present high c values. Note that: i) the $\sqrt{f/c}$ ratio is a measure of the distance between polymer chains, and ii) the previously mentioned concepts apply to dense polymers where the interchain distance is of the order or smaller than the penetrant size so that the penetrant diffusion is controlled by voids formed by the thermally activated motion of the polymer chain segments. Combining the previous relations, the following equation can be obtained for the penetrant diffusivity:

$$lnD_i = -\left(\frac{1-a}{RT}\right)cd_i^2 + f\left(\frac{1-a}{RT}\right) - b \tag{16}$$

and the following relation for the diffusivity selectivity of the CO/CO_2 gas couple:

$$ln\frac{D_{CO}}{D_{CO_2}} = \left(\frac{1-a}{RT}\right)c\left(d_{CO_2}^2 - d_{CO}^2\right) \tag{17}$$

Eq. (12) only contains c as free parameter: we assume for it the value of 250 cal/(mol Å)^2, because experimental data in Fig. 4 reveal that the examined polymers have no diffusivity selectivity: considering that $d_{CO} = 3.76$ Å and $d_{CO_2} = 3.30$ Å we obtain $\frac{D_{CO}}{D_{CO_2}} =$, in line with the value provided by the experimental data in Fig. 5. However, such correlation, that is based purely on the molecular size, does not explain the higher than unity values of $\frac{D_{CO}}{D_{CO_2}}$ encountered in the literature.

It is noteworthy that the diffusion coefficient is expected to show an exponential behavior with the square of the molecular size (either kinetic or Lennard-Jones diameter) [130], although more sophisticated correlations have also been presented [136,137]. Molecular size of diffusing penetrant within polymers is also often estimated from the molar volume of the gas at the critical point V_c. Interestingly, V_c is equal to 90.1 cm^3/mol and 91.9 cm^3/mol [138], for CO and CO_2, respectively, indicating how these two molecules are similar for what concern their size. Furthermore, the diffusion of CO_2 is also affected by other factors, such as energetic interactions with the polymer groups, with respect to other gases, as also observed in other systems [139].

To summarize, diffusivity-selectivity for the CO_2/CO couple fluctuates in a very narrow range for all the polymers examined and is never far from unity. It thus seems that the ability of the different polymers to separate these two compounds does not depend on their intrinsic free volume and is not a function of the polymer structure.

The CO_2/CO selectivity of the examined membrane samples $\alpha_{CO_2,CO} = \frac{P_{CO_2}}{P_{CO}} = \left(\frac{D_{CO_2}}{D_{CO}}\right)\left(\frac{S_{CO_2}}{S_{CO}}\right)$ has thus solubility selective character because the values of the D_{CO_2}/D_{CO} ratio are, in all examined polymers, 1. Looking at Robeson's plots in Fig. 4 we can observe that the P_{CO_2}/P_{CO} values are more scattered than the D_{CO_2}/D_{CO} values thus reflecting more scattered S_{CO_2}/S_{CO} values, see Fig. 6 where we report the $\alpha_{CO_2,CO} = \frac{P_{CO_2}}{P_{CO}}$ selectivity values as a function of the $\left(\frac{S_{CO_2}}{S_{CO}}\right)$ solubility- selectivity values. Looking at the PE, PI and PU polymers, where a large set of data is present, and considering that $D_{CO_2}/D_{CO} = 1$, we can observe that S_{CO_2}/S_{CO} values range between an average value ~ 8 in polyimides and polyethylene to an average value ~ 20 in polyurethanes.

It's worthy to compare the reported solubility selectivity values with those predicted by the Freeman's model. The solution of small penetrants in solids is a two-step process consisting on: i) the condensation of the gas penetrants to form liquid-like aggregate, and ii) the mixing of the compressed penetrants with the polymer chain segments. The first step is controlled by the penetrant condensability while the second by the penetrant-polymer interaction [140]. Light gases interact with the polymer through weak forces (van der Waals) and, in absence of strong interactions with segments of the polymer chains such as hydrogen bonding, the first term dominates. In this situation, the penetrant solubility scales with penetrant parameters measuring its condensability

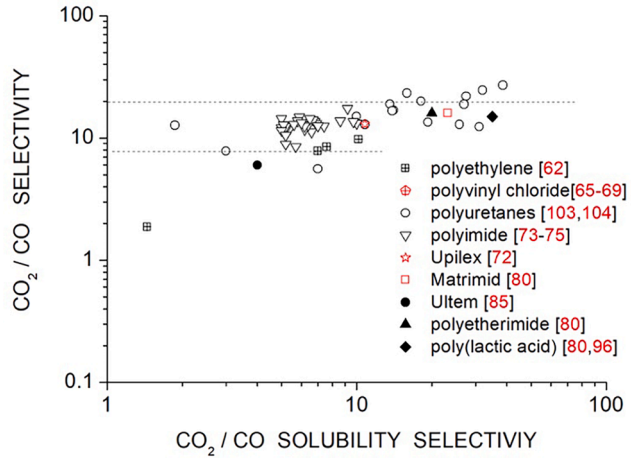

Fig. 6. Experimental P_{CO2}/P_{CO} selectivity values as a function of the S_{CO2}/S_{CO} solubility-selectivity values data measured at near ambient temperature in different polymers.

such as critical temperature T_C or Lennard-Jones temperature ε/k_B[140].

Models provide for penetrant solution in polymers the following relation with the Lennard-Jones temperature [141,142]:

$$\ln(S_0) = M + N(\varepsilon/k_B) \tag{18}$$

where the S_0 term is the gas solubility at infinite dilution in $cm^3(STP)/cm^3_{pol}atm$ units. The fitting of solubility data obtained at near ambient temperatures for a large number of glassy and rubbery polymers by eq. (13) was carried out by Robeson which obtained a value of $M = -7.30$ and $N = 0.0249\ K^{-1}$ [143]. Eq. (17) provides the following relation for the solubility- selectivity:

$$\frac{S_{CO_2}}{S_{CO}} = e^{N\left(\frac{\varepsilon_{CO_2}}{k_B} - \frac{\varepsilon_{CO}}{k_B}\right)} \tag{19}$$

Considering a Lennard-Jones temperature of 189 and 100 K for CO_2 and CO, respectively, the expected $\frac{S_{CO_2}}{S_{CO}}$ values is ~ **6**.

An alternative empirical correlation, that was also formalized into the Lattice Fluid and the Non-Equilibrium Lattice Fluid models, is given by [144]:

$$\ln(S_0) = A + BT_C \tag{20}$$

where the parameter B is a constant with value $0.016\ K^{-1}$ while the value of the A parameter depends on penetrant-polymer interaction and polymer free volume: when penetrant-polymer interactions are negligible A assumes the value of − 9.7 and − 8.7 in rubbery and glassy polymers, respectively [56,144–146]. The following solubility- selectivity relation can be obtained:

$$\frac{S_{CO_2}}{S_{CO}} = e^{B\left(T_{C,CO_2} - T_{C,CO}\right)} \tag{21}$$

Considering T_C values of 304.1 K for CO_2 and 133.2 K for CO, eq. (20) provides solubility- selective values ~ **18**.

Therefore, both the empirical correlations indicate values consistent with the experimental ones. Furthermore, experimental data for solubility-selectivity lie within a very narrow range, indicating that the separation of this gas mixture is not a strong function of the polymer nature and type. On the other hand, the absolute permeability can vary across several orders of magnitude depending on the polymer free volume.

It is therefore possible to pick polymers with relatively good permeability without compromising dramatically the selectivity as the trade-off mechanism seems to be rather mild for this couple of gases. The reason lies in the fact that the diffusion or size separation mechanism does not play a role as it does in other separations, with the main selective role assigned to the different condensability of the two penetrants. The addition of polar and CO_2-philic components to the polymer shifts the separation to higher selectivity, as in the case of PEGMA matrices, but the value seldom exceeds 30. Given the strong dependence of this separation on solubility, we believe that the polymeric membranes may become attractive at low temperatures and if a proper functionalization with the polymeric membrane with CO_2-attracting groups such as aminic functionalities is performed, as in the case of facilitated CO_2 transport.

Finally, it is worth to mention that the permeability of CO_2 and CO, like that of other gases, can be estimated from the properties of pure penetrants and pure polymers, by using dedicated correlations based, among the others, on group contribution approaches [147,148], thermodynamic and transport models [149], or machine learning algorithms [150].

4.2. *Effect of temperature on the CO_2/CO separation*

It is interesting to inspect the effect the operative temperature can play in the CO_2/CO separation performances of the examined polymeric membrane. To this task, the key parameters are the activation energies for CO_2 and CO transport, which are presented in Table 12, as retrieved from the literature for the polymers analyzed. It can be clearly seen that for all reported polymers the activation energy for permeation E_P is larger for CO than for CO_2, in some cases significantly, indicating that the separation performances of the polymeric membranes worsen with temperature. Conversely, the activation energy for diffusion E_D is often comparable for the two penetrants.

The observed temperature behaviors are in line with what discussed above. CO_2 and CO, indeed, are characterized by similar kinetic diameters and comparable diffusivity values, but also similar thermal behavior and E_D values, as expected from Eq. (15) [122]. The differences in E_P arises from the different effect of temperature on solubility, described by the sorption enthalpy ($\Delta H_s = E_P - E_D$) in Eq. (1). Its value is expected to decrease linearly with the Lennard-Jones square well parameter ε/k, which is significantly larger for CO_2 than for CO (ε/k_B = 91.7 K for CO and ε/k_B = 195.2 K for CO_2), as discussed by van Amerongen [130].

Table 12
Activation energy values for permeation (E_P) and diffusion (E_D) for CO_2 and CO. (*): Dried at 170 °C, 10 h in vacuum. (**): Annealed at 170 °C, 3 h in N_2 flow. (***): Annealed at 300 °C, 2 h in N_2 flow.

Polymer	E_P^{CO2} (kJ/mol)	E_P^{CO} (kJ/mol)	E_D^{CO2} (kJ/mol)	E_D^{CO} (kJ/mol)
PE (Grex) [62]	30.1	39.3	35.5	36.8
PE (Alathon 14) [62]	38.9	46.4	38.5	39.7
Hydropol [62]	36.4	44.7	36.8	37.2
Natural rubber [62]	21.7	30.9	34.3	30.9
PI (BPDA;ODA) (*) [72]	16.1	–	34.4	–
PI (BPDA;ODA) (**)	21.3	–	38.4	–
PI (BPDA;ODA) (***)	22.2	–	39.5	–
BPDA-DDS [73]	12.4	–	28.9	–
BPDA-DDBT [73]	6.7	–	23.2	–
Matrimid® [80]	7.7	20.7	32.5	28.7
Matrimid® [81]	8.1	16.5	–	–
Kapton® [83]	17.4	28.4	–	–
Ultem® [85]	34.7	78.7	–	–
PEI [80]	1.0	9.3	20.0	21.9
PDMS [92]	− 2.4	7.8	–	–
PDMS [53]	2.2	11.0	–	–
Pebax® 2533 [92]	6.5	19.4	–	–
PTMSP [53]	− 6.5	− 2.1	–	–
PLA [80,96]	22.4	36	39	47

The activation energy values obtained for the two penetrants and for the various polymers, coupled to the corresponding permeability data at near room temperature reported in the previous tables were used to estimate the behavior of the permeability-selectivity performances of selected systems in a quite wide temperature range, spanning from −20 up to 100 °C. Such trends are reported in Fig. 7, compared with the Robeson upper-bound proposed for such separation for some polymer membranes.

The graph shows clearly how it is possible to improve the performance of the membranes by reducing the temperature, exploiting the rather different values for the activation energy of permeation of *CO* and CO_2. The lines representing the trend of separation performance with decreasing temperature are characterized by a slope, in absolute value, significantly larger than that of the upper bound, which is eventually crossed for some polymers at the lowest temperature value considered (− 20 °C). Such an effect seems to be more pronounced for rubbery polymers (PDMS and PEBAX in particular) or ultra-high free volume glasses (PTMSP) for which the E_P for CO_2 is very small or even negative.

4.3. Summary of factors affecting the membrane performance

In this section we review the main factors which may be tuned to optimize the membrane performance.

1. **Polymer FFV:** the polymer fractional free volume affects positively the permeability without dramatically reducing the selectivity, due to the mild tradeoff effect experienced for this mixture and the weak diffusivity-selectivity.
2. **Polymer nature:** being this separation highly reliant on solubility of CO_2, the presence of polymer groups which interact strongly with CO_2 has a positive effect both on permeability and selectivity
3. **Temperature:** as shown in Fig. 6, decreasing the temperature down to −20 °C has always a positive effect on selectivity. The effect on permeability varies with the polymer type, being positive in the case of polymers like PDMS and PTMSP, weakly negative in the case of PEI, Pebax and Matrimid, and strongly negative in the case of PE Grek, natural rubber and Kapton, where the difference between the E_P values of *CO* and CO_2 is highest.
4. **Humidity:** the effect of humidity on the separation of this mixture was not analysed in the literature, but we can predict that moisture may trigger competition effects and reduce the solubility of both gases.

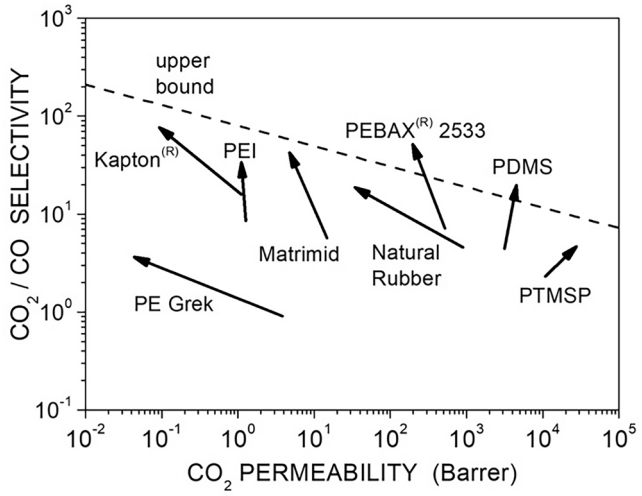

Fig. 7. Perm-selectivity performances of selected polymers, calculated in the temperature range − 20 to + 100 °C from room temperature permeability data and activation energies for permeation (Table XIII). The arrow for each polymer points to the lower temperature direction.

4.4. Simulation of a single stage membrane separation unit

The membrane performances analyzed in detail in terms of permeability and selectivity of the CO_2/CO couple were then used to simulate the possible output from a membrane unit, working in crossflow configuration. To this aim, a simple modeling approach may be considered, coupling the transport equation for each species to the mass balance. For a simple binary mixture, the transport of each species *i* across the membrane at steady state is related to the logarithmic mean of the partial pressure gradient $\frac{\Delta p_{i,ML}}{l}$, in analogy to a heat exchanger in crossflow configuration, as follows [151]:

$$J_i = P_i \frac{\Delta p_{i,ML}}{l} \tag{22}$$

The model is implemented in order to evaluate the performances of a hypothetical membrane of a certain area A, fabricated as thin film (active layer thickness considered 1 μm), subject to a certain pressure drop. For simplicity sake, a binary CO_2/CO mixture is considered as feed (10 Nm^3/h), characterized by a 29 % molar concentration of carbon monoxide, as suggested by the upstream plasma-assisted process that creates the mixture [83]. The model provides the molar fluxes of each component in the two streams exiting the membrane separator, and is used to evaluate the main key performance indicators for the separation: i) CO_2 recovery (CO_2 molar flux in the permeate/CO_2 fed); ii) *CO* recovery (*CO* molar flux in the retentate/*CO* fed); iii) CO_2 purity in the permeate; and iv) *CO* purity in the retentate.

Four different polymers are considered, namely PC-ES 2000 Polyurethane, Cellulose Acetate, Pebax®-1657 and PDMS, aiming to span from rubbery to glassy polymers as well as from conventional to innovative membrane materials, and test the effect of rather different CO_2 permeability values. Near room temperature permeability properties of the polymers are accounted for (35 °C) and retrieved from the tables above reported. Although two different pressures were considered, Fig. 8 reports only the results obtained at the highest differential pressure applied, 10 bar for PC-ES 2000 PU, Cellulose Acetate and Pebax®-1657, and 5 bar for PDMS (due to its outstanding permeability values). However, the comparison with a lower value of transmembrane pressure is included in the Supplementary Information Section.

The results obtained indicate there is a reasonable range of membrane area that allows a separation of the two components with quite large recovery of both CO_2 and *CO* (around 90 % or above) with good purities (about 90 %). Such value may be identified around 25 m^2 for PC-ES2000 membrane, at 100 m^2 for CA, characterized by quite large selectivity values. Conversely, the more permeable (but less selective) rubbery membranes require a smaller value of active area about 12 m^2 for Pebax, while the very large permeability of PDMS leads to very small membrane areas (0.2–0.3 m^2), but the separation process in this case is not very effective, and it can be considered useful only if coupled with other stages.

Such analysis is not meant to be exhaustive, but it aims to provide some qualitative indication on the feasibility of such separation by membranes. Further developments are required to identify a strategy for the whole process, integrating the reaction unit, evaluating the possibility to recycle carbon dioxide and identifying a downstream use for the carbon monoxide produced. Such aspects will allow to identify in more detail target parameters, i.e. purity and recovery, of the key components from the membrane unit, and guide the selection of the membrane material and operative conditions. The presence of other components, such as oxygen or other impurities, should also be considered.

5. Conclusions

In this review we have analyzed the data relative to CO_2 and *CO* transport, sorption and diffusion into different families of polymers varying by chemical nature and microstructure. Such analysis is moti-

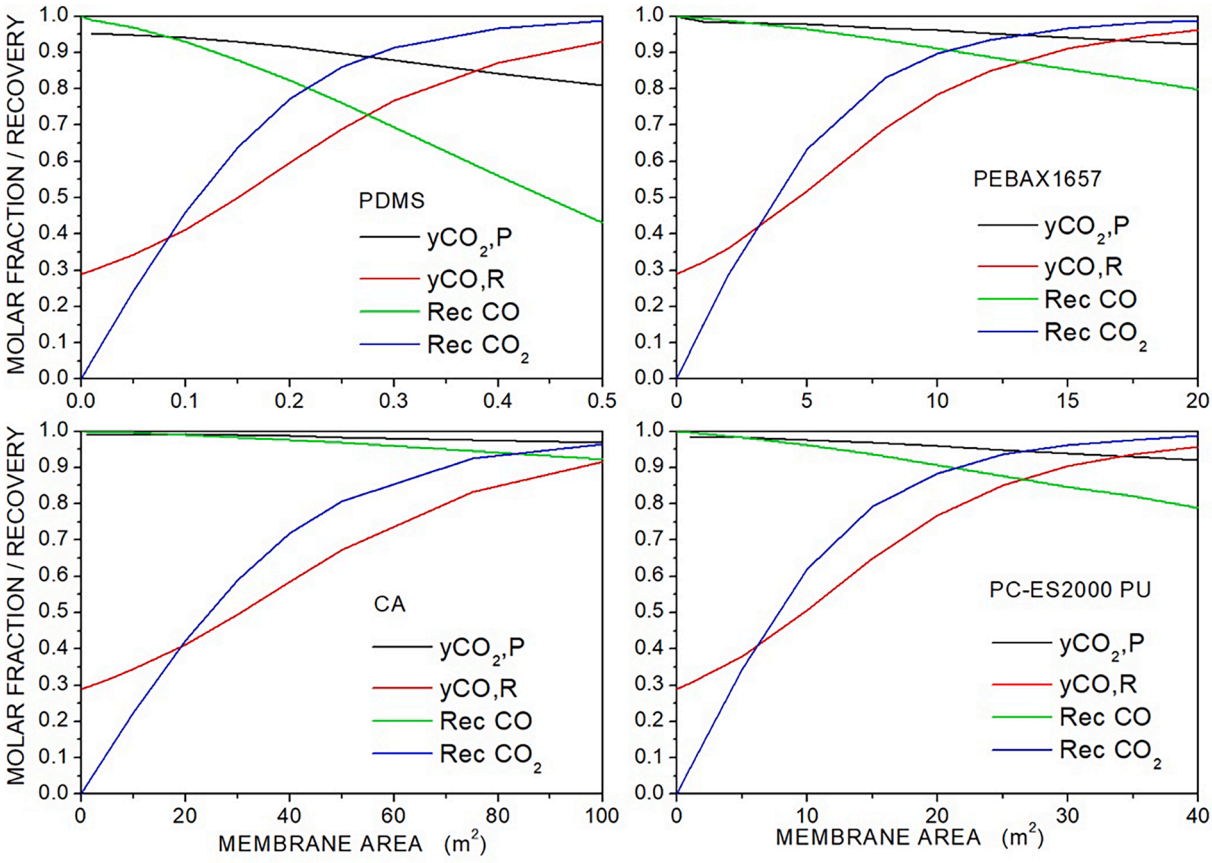

Fig. 8. Results of the membrane process simulations at 35 °C obtained with PDMS, CA, Pebax1657 and PC-ES2000 at 10 bar differential pressure (5 bar for PDMS only), in terms of CO_2 and *CO* recovery, as well as CO_2 and *CO* purity in the feed and retentate streams, respectively, as function of active membrane area (reference thickness 1 μm) for a 10 Nm^3/h CO_2/CO feed (29 mol.% of *CO*).

vated by the recent interest in the plasma-mediated reaction of CO_2 splitting to *CO* and O_2, which is an interesting conversion route for this greenhouse gas. Membrane can be used to purify the reaction products and adjust the composition of the mixture for further processing and conversion stages of the *CO*.

The literature review reveals a lack of homogenous sets of data for *CO* and CO_2, but despite this, the results highlighted by this review are extremely clear and unambiguous. We have noticed that all polymers tested in the literature are more permeable to CO_2 than to *CO*, making the membrane separation process favorable if a retentate stream enriched in *CO* is the desired outcome. While the permeability can be varied across a rather significant range by changing the polymer type, the same cannot be said for the selectivity, which is bound by a very limited, or even unfavorable, diffusivity contribution: indeed, despite the moderately larger size of *CO* with respect to CO_2, the diffusivity of the first gas is often larger than that of the latter. Therefore, the CO_2/CO selectivity value is sorption-controlled. Based on the different condensabilities of the two gases and empirical correlations, the selectivity should assume values between 6 and 18 for this couple, which is indeed close to the average value observed experimentally which mostly lie between 7 and 20 with few exceptions. In general, the selectivity oscillates within a very narrow range, with a very weak tradeoff mechanism observed, corresponding to a small absolute value of the upper bound slope. A CO_2/CO upper bound relationship was proposed considering all the data reported in this work: materials that lie closer to this limit are Cellulose Acetate, PEGMA-based and PEBAX copolymers. Given the nature of this separation, it is likely that facilitated transport may help achieve excellent separation performance above the upper bound. The effect of temperature is unfavorable for the selectivity, because the permeation of *CO* increases more than that of CO_2 by increasing the temperature, due to the large negative heat of sorption of this latter gas, so that better performances, as reported in the review, would be obtained when cooling the feed mixture. A preliminary estimate of the purification and recovery degrees obtainable in 4 selected polymers in standard operative conditions gives encouraging results as the membrane may operate flexibly in combination with other units of the *CO* conversion routes, e.g. the reactor and the post-utilization of *CO*.

In conclusion, membranes seem a viable separation technology to carry out this separation and can be coupled to *CO* utilization strategies as non-thermal plasma mediated *CO* splitting that occurs in such conditions. One of the most important influencing factors for the membrane-based separation of this mixture is the temperature: low temperatures favor the selectivity. On the material side, a selectivity improvement could be obtained by enhancing the solubility-selectivity of the polymer, adding CO_2 – philic groups to the membrane to avoid loss of *CO* in the permeate stream.

CRediT authorship contribution statement

Riccardo Checchetto: Writing – review & editing, Writing – original draft, Investigation, Formal analysis, Data curation, Conceptualization. **Maria Grazia De Angelis:** Writing – review & editing, Supervision, Methodology, Conceptualization. **Matteo Minelli:** Writing – review & editing, Software, Methodology, Investigation, Data curation.

Declaration of competing interest

The authors declare that they have no known competing financial interests or personal relationships that could have appeared to influence the work reported in this paper.

Data availability

Data will be made available on request.

Appendix A. Supplementary material

Supplementary data to this article can be found online at https://doi.org/10.1016/j.seppur.2024.127401.

References

[1] P.A. Redhead, J.P. Hobson, E.V. Kornelsen, The Physical Basis of Ultrahigh Vacuum, American Institute of Physics, New York, 1993.

[2] J. Bierhals, Carbon Monoxide, Ullmann's Encyclopedia of Industrial Chemistry (Wiley-VCH, Weinheim (2005), https://doi.org/10.1002/14356007.a05_203; ISBN: 978-3527306732.

[3] M. Martin Martin, *Syngas*, in *Industrial Chemical Process Analysis and Design*, M. Martin Martin Ed. (2016, Elsevier, Amsterdam), pp. 199-297.

[4] Ce Du, Peng Lu, and N. Tsubaki, Efficent and new production methods of chemical and liquid fuels by carbon monoxide hydrogenation, ACS Omega **5** (2020) 49-56.

[5] E. Friedler, G. Grossman, D. B. Keserbohm, G. Weiss and C. Witte, Methanol, Ullmann's Encyclopedia of Industrial Chemistry (Wiley-VCH, Weinheim, 2005), 10.1002/14356007.a16_465; ISBN: 978-3527306732.

[6] W. Schneider, W. Diller, Phosgene, Ullmann's Encyclopedia of Industrial Chemistry (Wiley-VCH, Weinheim, 2005), 10.1002/14356007.a19_411; ISBN: 978-3527306732.

[7] L.E. Heim, H. Konnerth, M.H.G. Prechtl, Future perspectives for formaldehyde: pathways for reductive synthesis and energy storage, Green Chem. 19 (2017) 2347–2355.

[8] J.F. Roth, The production of acetic acid, Platinum Metals Rev. 19 (1975) 12–14.

[9] Min Hu, C. Jacobsen Eds, Oxidative stability and shelf life of foods containing oils and fats, 2016 AOCS Press published by Elsevier Inc.; ISBN: 978-1-63067-056-6, doi.org/10.1016/C2015-0-00077-6.

[10] S. E. Woverton Ed., Comprehensive Dermatologic Drug Therapy (Elsevier, 2013), 10.1016/B978-1-4377-2003-7.00076-5, ISBN: 978-1-4377-2003-7.

[11] S.W.W. Ryter, A.M.K. Choi, Carbon monoxide in exhealed breath testing and therapeutics, J. Breath Res. 7 (2013) 017111.

[12] R. Ma, B. Xu and X. Zhang, Catalytic partial oxidation (CPOX) of natural gas and renewable hydrocarbons/oxygenated hydrocarbons – a review, Catal. Today 338 (2019) 18-30. R. L. Keiski, S. Ojala, M. Huuhtanen, T. Kolli, K. Leiviska, Partial oxidation processes and technologies for clean fuel and chemical production, Adv. Clean Hyrocarbon Fuel Processing – Sci. Technol. Woodhead Publishing Series in Energy (2011) 262-286, S. Sengodan, R. Lan, J. Humphreys, D. Du, W. Xu, H. Wang and S. Tao, Advances in reforming and partial oxidation of hydrocarbons for hydrogen production and fuel cell applications, Renew. Sustain. Energy Rev. 82 (2018) 761-780.

[13] T.Y. Amifi, K. Ghasemzageh and A. iulianelli, Membrane reactors for suistanable hydrogen production through steam reforming of hydrocarbons: a review, Chem. Eng. Proc. Process Intensification **157** (2020) 108148; G. Guam, M. Kaewpanha, X. Hao and A. Abudula, Catalytic steam reforming of biomass tar: prospect and challenges, Renew. Sustain. Energy Reviews 58 (2016) 450-461.

[14] H. Boerrigter, R. Rauch, Handbook Biomass Gasification, (Biomass Technology Group, 2005).

[15] C. Higman, M.v.d. Burgt, Gasification, Elsevier Science, Amsterdam, 2008.

[16] Yongxiang Yin, Tao Yang, Zhikai Li, Edwin Devid, D. Auerbachce and Aart W. Kleyn, CO_2 conversion by plasma: how to get efficient CO_2 conversion and high energy efficiency, Phys.Chem.Chem.Phys. **23** (2021) 7974.

[17] B. Ashford, Xin Tu, Non-thermal plasma technology for the conversion of CO_2, Curr. Opin. Green Sustain. Chem. **3** (2017) 45-49.

[18] S.M.W. Wilson, D.A. Kennedy, F.H. Tezel, Adsorbent screening for CO_2/CO separation for applications in syngas production, Sep. Purif. Technol. 236 (2020) 116268.

[19] N.N. Dutta, G.S. Patil, Developments in CO separation, Gas Sep. Purif. **9** (11195) 277-283.

[20] X. Ma, J. Albertsma, D. Gabriels, R. Horst, S. Polat, C. Snoeks, F. Kapteijn, H. B. Eral, D.A. Vermaas, B. Mei, S. de Beer, M.A. van der Saar, Carbon monoxide separation: past, present and future, Chem. Soc. Rev. 52 (2023) 3741–3777.

[21] Linde Engineering, Partial condensation process and liquid methane wash, https://www.linde-engineering.com/en/processplants/hydrogen_and_synthesis_gas_plants/gas_processing/partial-condensation_process_and_liquid_methane_wash/index.html.

[22] J.A. Hogendoorn, W.P.M. van Swaaij, G.F. Versteeg, The absorption of carbon monoxide in COSORB solution: absorption rate and capacity, Chem. Eng. J. 59 (1995), 343-252.

[23] S.E. Repper, A. Haynes, E.J. Ditzel, G.J. Sunley, Infrared spectroscopic study of absorption and separation of CO using copper(I)-containing ionic liquids, Dalton Trans. 46 (2017) 2821–2828.

[24] D. Tao, F. Chen, Z. Tian, K. Huang, S.M. Mahuin, D. Jiang, S. Dai, Highly efficient carbon monoxide capture by carbanion- functionalized ionic liquid through C-site interaction, Angew. Chem. 129 (2017) 6947–6951.

[25] D.M. Ruthven, Principles of Adsorption and Adsorption processes, John Wiley, New York, 1984.

[26] S. Koizumi, T. Fujita, T. Sukuraia, Installation and operation of high purity CO gas recovery plant, Kawasaki Steel Technical Report 16 (1987) 107–113.

[27] F. Kasuya, T. Tsuji, High purity CO gas separation by pressure swing adsorption, Gas Sep. Purif. 5 (1991), 242-242.

[28] M.W.S. Wilson, A.D. Kennet, F.H. Tezel, Adsorbent screening for CO2/CO separation for applications in syngas separation, Sep. Purif. Technol. 236 (2020) 116268.

[29] H. Sato, W. Kosaka, R. Matsuda, A. Hori, Y. Hijkata, R. V. Belosludov, S. Sakaki, M. Takata, S. Kitagawa, Self-acceleratiomg CO sorption in soft nanoporous crystal, Science 343 (2014) 167-170. Y.T. Wang, S. Jalife, A. Robles, M. Deric, J.I. Wu, W. Kaveevivitchai, O. S. Milianic, T.H. Chen, Efficient CO_2/CO separation by pressure swing adsorption using an intrinsically nanoporous molecular crystal, ACS Appl. Nano Mater. **5** (2022) 14021-14026.

[30] A. Evans, R. Luebke, C. Petit, The use of metal-organic frameworks for CO purification, J. Mater. Chem. A 6 (2018) 10570–10594.

[31] E.D. Bloch, M.R. Hudson, J.A. Mason, S. Chavan, V. Crocella, J.D. Howe, K. Lee, A.L. Dzubak, W.L. Queen, J.M. Zadrozny, S.J. Geier, L.C. Lin, L. Gagliardi, B. Smith, J.B. Neaton, S. Bordiga, C.M. Brown, J.R. Long, Reversible CO binding enables tunable CO/H_2 and CO/N_2 separation in metal-organic frameworks with exposed divalent metal cations, J. Am. Chem. Soc. 136 (2014) 10752–10761.

[32] Y. Yin, Z.H. Wen, X.Q. Liu, L. Shi, A.H. Yuan, Modification of metal organic framework HKUST-1 with CuCl for selective separation of CO/H2 and CO/N2, J. Porous Mater. 25 (2018) 1513–1519.

[33] S.D. Kenarsari, D. Yang, G. Jiang, S. Zhang, J. Wang, A.G. Russel, Q. Wei, M. Fan, Review of recent advances in carbon dioxide separation and capture, RCS Adv. 3 (2013) 22739–22773.

[34] A. Brunetti, P. Bernardo, G. Barbieri, Membrane Engineering: Progress and Potentialities in gas Separation, in: Y. Yampolskii, B. Freeman (Eds.), Membrane Gas Separation, John Wiley and Sons, Chichester, 2010, p. 281.

[35] A.F. Ismail, K.C. Khulbe, T. Matsuura, Gas Separation Membranes (Springer International Publishing, Switzerland, 2015, pp. 241-287).

[36] Air Products and Chemical Inc., Advanced Prism Membrane System for Cost Effective Gas Separation, 1999.

[37] S.P. di Martino, J.L. Glazer, C.D. Houston, M.E. Schott, Hydrogen/carbon monoxide separation with cellulose acetate membranes, Gas Sep. Purif. 2 (1988) 120–125.

[38] R.W. Baker, B.T. Low, Gas separation membrane materials: a perspective, Macromolecules 47 (2014) 6999–7013.

[39] M.F. San Roman, E. Bringas, R. Ibanez, I. Ortiz, Liquid membrane technology: fundamentals and applications, J. Chem. Technol. Biotechnol. 85 (2010) 2–10.

[40] G. Zarca, I. Ortiz, A. Urtiaga, Copper(I)-containing supported ionic liquid membranes for carbon monoxide/nitrogen separation, J. Membrane Sci. 438 (2013) 38–45.

[41] S. Feng, Y. Wu, J. luo and Y. Wan, $AgBF_4$/[emim][BF_4] supported ionic liquid membrane for carbon monoxide/nitrogen separation, J. Energy Chem. **29** (2019) 31-39.

[42] Y. Han, W.S. Winston Ho, Polymeric membranes for CO_2 separation and capture, J. Membrane Sci. 628 (2021) 119244.

[43] Linfeng Lei, Lu bai, Arne Lindbrathen, Fengjiao Pan, Xiangping Zhang and Xuezhong He, Carbon membranes for CO_2 removal: Status and perspectives from materials to processes, Chem. Eng. Journal **401** (2020) 126084.

[44] Z.i. Tong, A.K. Sekizkardes, Recent developments in high-performance membranes for CO_2 separation, Membranes 22 (2021) 156.

[45] K. Ramasubramanian, H. Verweij, W.S. Winston Ho, Membrane processes for carbon capture from coal-fired plant flue gas: a modeling and cost study, J. Membrane Sci. 421–422 (2012) 299–310.

[46] V. Vakharia, K. Ramasubramanian, W.S.W. Ho, An experimental and modeling study of CO2-selective membranes for IGCC syngas purification, J. Membrane Sci. 488 (2015) 56–66.

[47] J.D. Wind, D.R. Paul, W.J. Koros, Natural gas permeation in polyimide membranes, J. Membrane Sci. 228 (2004) 227–236.

[48] W. Yave, A. Car, Polymeric membranes for post-combustion carbon dioxide (CO2) capture, in: A. Basile, S.P. Nunes (Eds.), Advanced membranes Science and Technology for Sustainable Energy and Environmental Applications, (Woodhead Publishing Series in Energy, Cambridge, 2011, pp. 160–183.

[49] T.C. Merkel, M. Zhou, R.W. Baker, Carbon dioxide capture with membranes at IGCC power plant, J. Membrane Sci. 389 (2012) 441–450.

[50] R.P. White, J.E.G. Lipton, Polymer free volume and its connection to the glass transition temperature, Macromolecules 49 (2016) 3987–4007.

[51] J. Sharma, K. Tewari and R. K. Arya, Diffusion in Polymers – A review on the free volume theory, Prog. Organic Coat. **111** 82017) 83-92.

[52] N.R. Horn, A critical review of free volume and occupied volume calculation methods, J. Membrane Sci. 518 (2016) 289–294.

[53] J.G. Wijmans, R.W. Baker, The solution-diffusion model: a review, J. Membrane Sci. 107 (1995) 1–21.

[54] S. Matteucci, Y. Yampolskii, B. D. Freeman and I. Pinnau, Transport of Gases and Vapors in Glassy and Rubbery Polymers, in "Materials Science of Membranes for Gas and Vapor Separation", Y. Yampolskii, I, Pinnau and B. D. Freeman Eds. (2006, John Wiley & Sons Ltd., ISBN: 0-470-85345-X).

[55] Y. Yampolskii, Permeability of polymers, in: Y. Yampolskii and E. Finkelstein (Eds.), Membrane materials for Gas and Vapor Separation: synthesis and application of silicone-containing polymers, John Wiley and Sons, Chichester, 2017, pp. 1-15.

[56] P. Maeres, The diffusion of gases through poly-vinyl acetate, J. Am. Chem. Soc. 76 (1954) 3415–3422.

[57] L.M. Robeson, The upper bound revisited, J. Membrane Sci. 320 (2008) 390–400.

[58] L.M. Robeson, Z.P. Smith, B.D. Freeman, D.R. Paul, Contributions of diffusion and solubility selectivity to the upper bound analysis for glassy gas separation membranes, J. Membrane Sci. 453 (2014) 71–83.

[59] L.M. Robeson, Correlation of separation factor versus permeability for polymeric membranes, J. Membrane Sci. **62** (1991) 165–185; L.M. Robeson, W.F. Borgoyne, M. Langsam, A.C. Savoca, C.F. Tien, High performance polymers for membrane separation, Polymer **35** (1994) 4970–4978.

[60] B.D. Freeman, Basis of permeability/selectivity tradeoff relations in polymeric gas separation membranes, Macromolecules 32 (1999) 375–380.

[61] W. Porsch, Polyolefins, in Applied Plastics Engineering Handbook (Elsevier, Oxford, 2017), pp. 27-53.

[62] A.S. Michaels, H.J. Bixler, Flow of gases through polyethylene, J. Polymer Sci. 1 (1961) 413–419.

[63] O. Atiq, E. Ricci, M.G. Baschetti, M.G. De Angelis, Modelling solubility in semi-crystalline polymers: a critical comparative review, Fluid Phase Equilib. 556 (2022) 113412.

[64] M. Minelli, M.G. De Angelis, An equation of state (EoS) based model for the fluid solubility in semicrystalline polymers, Fluid Phase Equilib. 367 (2014) 173–181.

[65] M.D. Sefcik, J. Schaefer, F.L. May, D. Raucher, S.M. Dub, Diffusivity of gases and main-chain cooperative motions in plasticized poly(vinyl chloride), J. Polym. Sci. Polym. Phys. 21 (1983) 1041–1054.

[66] D.W. Brubaker, K. Kammermeyer, Flow of gases through plastic membranes, Ind. Eng. Chem. 45 (1953) 1148–1152.

[67] P. Tiemblo, J. Guzman, E. Riande, C. Mijangos, H. Reinecke, The gas transport properties of PVC functionalized with mercapto pyridine groups, Macromolecules 35 (2002) 420–424.

[68] Seung Hyeon Yeon, Sung Hoon Ahn, Jong Hak Kim, Ki Bong Lee, Yujin Jeong and Seong Uk Hong, Synthesis and gas permeation properties of poly(vinyl chloride)-graft-poly(vinyl pyrrolidone) membranes, Polym. Adv. Technol. **23** (2012) 516–521.

[69] R. L. Ballard, The sorption and transport of carbon dioxide and methane in plasticized poly(vinyl chloride), University of Cincinnati, 1992, Ph.D. Dissertation (ProQuest).

[70] Shi-Yong Yang and Li-Li Yuan, Advanced Polyimide films, in Advanced Polyimide Materials, Synthesis, Characterization and Applications, Shi-Yong Yang Ed. (Elsevier, Amsterdam, 2018), pp. 1-66.

[71] Y. Xiao, B.T. Low, S.S. Hosseini, T.S. Chung, D.R. Paul, The strategies of molecular architecture and modification of polyimide- based membranes for CO_2- removal from natural gas, Prog. Polym. Sci. 34 (2009) 561–580.

[72] K. Tanaka, H. Kita, K. Okamoto, A. Nakamura, Y. Kusuki, The effect of morphology on gas permeability and permeselectivity in polyimide based on 3,3',4,4'-Biphenyltetracarboxylic Dianhydride and 4,4'-Oxydianiline, Polym. J. 21 (1989) 127–135.

[73] K. Tanaka, H. Kita, K. Okamoto, A. Nakamura, Y. Kusuki, Gas permeability and permselectivity in polyimides based on 3,3',4,4'- biphenyltetra-carboxylic dianhydride, J. Membrane Sci. 47 (1989) 203–215.

[74] K. Tanaka, H. Kita, M. Okano, K. Okamoto, Permeability and perselectivity of gases in fluorinated and non-fluorinated polyimides, Polymer 33 (1992) 582–585.

[75] K. Tanaka, M. Okano, H. Toshino, H. Kita, K. Okamoto, Effect of methyl-substituents on permeability and permselectivity of gases in polyimide prepared from methyl-substituted phenylenediamines, J. Polym. Sci. Part B: Polym. Physics 30 (1992) 907–914.

[76] Chae-Young Park, Eun-Hee Kim, Jong Hak Kim, Young Moo Lee, Jeong-Hoon Kim, Novel semi-alicyclic polyimide membranes: synthesis, characterization, and gas separation properties, Polymer **151** (2018) 325-333.

[77] D.F. Sanders, Z.P. Smith, R. Guo, L.M. Robeson, J.E. McGrath, D.R. Paul, B. D. Freeman, Energy-efficient polymeric gas separation membranes for a sustainable future: a review, Polymer 54 (2013) 4729–4761.

[78] www.ube.com/upilex/en/catalog.html#cata_upilex.

[79] X.Y. Chen, H. Vinh-Thang, A.V. Ramirez, D. Rodrigue, S. Kaliaguine, Membrane gas separation technologies for biogas upgrading, RCS Adv. 5 (2015) 24399–24448.

[80] R. Checchetto, M. Scarpa, M.G. De Angelis, M. Minelli, Mixed gas diffusion and permeation of ternary and quaternary CO2/CO/N2/O2 gas mixtures in Matrimid®, polyetherimide and poly(lactic acid) membranes for CO2/CO separation, J. Membrane Sci. 659 (2022) 120768.

[81] O.C. David, D. Gorri, A. Urtiaga, I. Ortiz, Mixed gas separation study for the hydrogen recovery from $H_2/CO/N_2/CO_2$ post combustion mixtures using a Matrimid membrane, J. Membrane Sci. 378 (2011) 359–368.

[82] F.P. McCandless, Separation of binary mixtures of CO and H_2 by permeation through polymeric films, Ind. Eng. Chem. Process Des. Develop. 11 (1972) 470–478.

[83] M. Hausladen, K.A. Lasala, C.R.F. Lund, Permeation through Kapton® polyimide at elevated temperatures, Chem. Eng. Comm. 143 (1969) 91–97.

[84] S. Carroccio, C. Puglisi, G. Montaudo, Polyetherimide, in Handbook of Engineering and Specialty thermoplastics Vol. 4, S. Thomas and P. M. Visakh (Eds.), (Wiley Online Library, 2011), pp. 79-110.

[85] F. Hamidavi, A. Kargari, A. Eliassi, Sorption and permeation study of polyetherimide/hydrophobica silica nanocomposite membrane for effective syngas(H2/CO/CO2) separation, Sep. Purif. Technol. 279 (2021) 119774.

[86] S.K. Rath, S.K. Sharma, K. Sudarshan, J.G. Chavan, T. U. Patro, P.K. Pujari, Subnanoscopic inhomogeneities in model end-cross linked PDMS probed by positron annihilation lifetime spectroscopy and their effects on thermomechanical properties, Polymer **101** (2016) 358-369, Wanpeng Liu, Yifan Li, Xiangxi Meng, Guanhua Liu, Shen Hu, Fusheng Pan, Hong Wu, Zhongyi Jiang, Baoyi Wang, Zhuoxin Li and Xingzhong Cao, Embedding dopamine nanoaggregates into a poly(dimethylsiloxane) membrane to confer controlled interactions and free volume for enhanced separation performance, J. Mater. Chem. A 1 (2013) 3717.

[87] V.P. Shantarovich, I.B. Kevdina, Y.P. Yampolskii, A.Y. Alentiev, Positron annihilation lifetime study of high and low free volume glassy polymers: effects of free volume sizes on the permeability and permselectivity, Macromolecules 33 (2000) 7453–7466.

[88] Asad Javaid, Membranes for solubility based gas separation applications, Chem. Eng. J. **112** (2005) 219-226; B. D. Freeman and I. Pinnau, Trends Polym. Sci. **5** (1997) 167.

[89] P.D. Sutrisna, J. Hou, H. Li, Y. Zhang, V. Chen, Improved operational stability of Pebax- based gas separation membranes with ZIF-8: a comparative study of flat sheet and composite hollow-fiber membranes, J. Membrane Sci. 524 (2017) 266–279.

[90] Yifan Li, Xueqin Li, Hong Wu, Qingping Xin, Shaofei Wang, Ye Liu, Zhizhang Tian, Tiantian Zhou, Zhongyi Jiang, Hongwei Tian, Xingzhong Cao and Baoyi Wang, *Anionic surfactant-doped Pebax membrane with optimal free volume characteristics for efficient CO_2 separation*, J. Membrane Sci. 493 (2015) 460-469; W. Yave and A. Car, Polymeric membrane for post- combustion carbon dioxide (CO_2) capture, in Science and Technology for Sustainable Energy and Environmental Applications, A. Basile and N. P. Nunes Eds. (Woodhead Publishing Science in Energy, 2011) p. 160-183.

[91] W. Yave, A. Car, K. V. Peinemann, M. Q. Shaikh, K. Ratzke and F. Faupel, Gas permeability and free volume in poly(amine-beta-ethylene oxide)/polyethylene glycol blend membranes, J. Membrane Sci. **339** (209) 177-183.

[92] B. Wilks, M.E. Rezac, Properties of rubbery polymers for the recovery of hydrogen sulfide from gasification gases, J. Appl. Polym. Sci. 85 (2002) 2436–2444.

[93] T.C. Merkel, R.P. Gupta, B.S. Turk, B.D. Freeman, Mixed-gas permeation of syngas components in poly(dimethulsiloxane) and poly(1-trymethylsilyl-1-propyne) at elevated temperature, J. Membrane Sci. 191 (2001) 85–94.

[94] Chae-Young Park, Bong-Jun Chang, Jeong-Hoo Kim and Young Moo Lee, UV-crosslinked poly(PEGMA-co-MMA-co-BPMA) membranes: synthesis, characterization and CO_2/N_2 and CO_2/CO separation, J. Membrane Sci. **587** (2019) 117167.

[95] N. More, M. Avhad, S. Utekar, A. More, Polylactic acid (PLA) membrane – significance, synthesis and applications: a review, Polymer Bulletin 80 (2023) 1117–1153; N.A.B. Taib, Md R. Rahman, D. Huda, K.K. Kuok, S. Hamdan, M.K.B. Bakri, M.R.M.B. Julahi, A. Khan, A review on poly lactic acid (PLA) as a biodegradable polymer, Polymer Bull. 80 (2023) 1179–1213.

[96] R. Checchetto, Accurate monitoring of gas mixture transport kinetics through polymeric membranes, Sep. Purif. Technol. 277 (2021) 119477.

[97] V. Vatanpour, M.E. Pasaoglu, H. Barzegar, O.O. Teber, R. Kay, M. Bastug, A. Khataee, I. Koyuncu, Cellulose acetate in fabrication of polymeric membranes: A review, Chemosphere 295 (2022) 133914.

[98] J. Feldman, I.W. Shim, M. Orchin, Permselectivity of cellulose acetate membranes; separation of H_2/CO mixtures and the effect of added transition metals, J. Appl. Polym. Sci. 34 (1987) 969–976.

[99] M. Najafi, M. Sadeghi, A. Bolverdi, M.P. Chenar, M. Pakizeh, Gas permeation properties of cellulose acetate/silica nanocomposite membranes, Adv. Polym. Tech. 37 (2018) 2043–2052.

[100] M. Golda-Cepa, K. Engvall, M. Hakkarainen, A. Kotarba, Recent progress on parylene C polymer for biomedical applications: a review, Prog. Org. Coat. 140 (2020) 105493.

[101] Y.S. Yeh, W.J. James, H. Yasuda, Polymerization of para-xylylene derivatives. VI. Morphology of parylene n and parylene c films investigated by gas transport characteristics, J. Polym. Sci.: Part B: Polym. Physics **28** (1990) 545-568.

[102] H. Janik, M. Sienkievicz and J. Kucinska-Lipka, Polyurethanes, in H. Dodiuk and S. H. Goodman Eds. Handbook of Thermoset Plastics (Elsevier, San Diego CA, 2014), pp. 253-295.

[103] M. Pecoraro, L. Zanderichi, A. Penati, F. Severini, F. Bianchi, Nanyun Cao, R. Sisto and C. Valentini, *Polyurethane membranes from polyether and polyester diols for gas fractionation*, J. Appl. Polym. Sci. **43** (1991) 687-697.

[104] N. Cao, M. Pegoraro, F. Bianchi, L. Di Landro, L. Zanderighi, Gas transport properties of Polycarbonate-Polyurethane membranes, J. Appl. Polym. Sci. 48 (1993) 1831–1842.

[105] J. Lv, Y. Cheng, Fluoropolymers in biomedical applications: state-of-the-art and future perspectives, Chem. Soc. Rev. 50 (2021) 5435.

[106] M. Mohr, D.R. Paul, Comparison of gas permeation in vinyl and vinylidene polymers, J. Appl. Polym. Sci. 42 (1991) 1711–1720.

[107] DuPont Tedlar® Polyvinyl Fluoride (PVF) Films General Properties, www.tedlar.com (2014).

[108] J. Maul, B.G. Frushour, J.R. Kontoff, H. Eichenauer, K. H. Ott, C. Schade, 2007, Polystyrene and Styrene Copolymers" in Ullmann's Encyclopedia of Industrial Chemistry, Wiley-VCH, Weinheim, doi:10.1002/14356007.a21_615.pub2.. C. Marquez, C. Martin, N. Linares and D. De Vos, Catalytic routes toward polystyrene recycling, Mater. Horiz. **10** (2023) 1625-1640.

[109] Permeability of polymers to gases and vapors, supplier technical report (P302-335-79, D306- 115-79). Dow Chemical Company; 1979.

[110] Polystyrol product line, properties, processing, supplier design guide (B 564e/2.93). BASF Aktiengesellschaft; 1993.

[111] Permeability of polymers to gases and vapors, supplier technical report (P302-335-79, D306- 115-79). Dow Chemical Company; 1979.

[112] L. De Vos, B. Van de Voorde, L. Van Daele, P. Dubruel, S. Van Vlierberghe, Poly (alkylene terephthalate)s: from current developments in synthetic strategies towards applications, Eur. Polym. J. 161 (2021) 110840.

[113] Mylar polyester film Product Information, DuPont Teijin Films, usa. dupontteijinfilms.com/wp-content/uploads/2017/01/Mylar_Chemical_Properties. (https://www.sandia.gov/polymer-properties/mylar-crystallinity/).
[114] E.L.V. Lewis, R.A. Duckett, I.M. Ward, J.P.A. Fairclough, A.J. Ryan, The barrier properties of polyethylene terephthalate to mixtures of oxygen, carbon dioxide and nitrogen, Polymer 44 (2003) 1631–1640.
[115] M. Mapes, H.C. Hseuh, W.S. Jiang, Permeation of argon, carbon dioxide, helium, nitrogen and oxygen through Mylar windows, J. Vac. Sci. Technol. A 12 (1994) 1699–1704.
[116] V.R. Sastri, High-temperature engineering thermoplastics: polysulfones, polyimides, polysulfides, polyketones, liquid crystalline polymers, fluoropolymers and polyarylamides (Elsevier, Oxford, 2022), pp. 233-286.
[117] O.S. Serbanescu, S.I. Voicu, V.K. Thakur, Polysulfone functionalized membranes: properties and challenges, Mater. Today Chem. 17 (2020) 100302; S. Kheirieh, M. Asghari, M. Afsari, Application and modification of polysulfone membranes, Rev. Chem. Eng. 34 (2018) 657-693, A.L. Khan, C. Klaysom, G. Amit, F. Ivo, J. Vankelecom, Polysulfone acrylate membranes containing functionalized mesoporous MCM-41 for CO_2 separation, J. Membrane Sci. 436 (2013) 145-153.
[118] J.S. McHattie, W.J. Koros, D.R. Paul, Gas transport properties of polysulphones: 1 Role of symmetry of methyl group placement on bisphenol rings, Polymer 32 (1991) 840–850.
[119] D. Nasarian, I. Salahshoori, M. Sadeghi, N. Rashidi, M. Hassanzadeganroudsari, Investigation of the gas permeability properties from polysulfone/polyethylene glycol composite membrane, Polymer Bull. 77 (2020) 5529–5552.
[120] C.A. Scholes, G.Q. Chen, G.W. Stevens, S.E. Kentish, Nitric oxide and carbon monoxide permeation through glassy polymeric membranes for carbon dioxide separation, Chem. Eng. Res. Des. 89 (2011) 1730–1736.
[121] J. Ahn, W.-J. Chung, I. Pinnau, M.D. Guiver, Polysulfone/silica nanoparticle mixed-matrix membranes for gas separation, J. Mem. Sci. 314 (2008) 123–133.
[122] Polyamides, Plastics in, E. C. Schule Ed., Encyclopedia of Polymer Science Technology (1st ed., Allied Chem. Corp., 2021), pp. 460–482.
[123] J. Ritz,H. Fuchs, H. Kiecza, W. C. Mora, "Caprolactam" Ullmann's Encyclopedia of Industrial Chemistry (Weinheim, Wiley-VCH), doi:10.1002/14356007.a05_031.pub2.
[124] F. Guisheng, L. Incarnato, L. Di Maio, D. Acierno, Discussion about the use of relative values of permeabilities between two gases for high molecular weight polymers, Polymer 36 (1995) 4345–4346.
[125] Y. Sakaguchi, H. Kawada, Y. Kato, Separation of H2 and CO through poly(sulfone-diamine) membranes, Kobunshi Ronbunshu 43 (1986) 755–759.
[126] Y. Sakaguchi, M. Tokai, H. Kawada, Y. Kato, Separation of H2 and CO through poly(sulfone-diamine) membranes. II. Highly permselective membranes containing bis(3-aminophenyl) sulfone as a diamine component, Polym. J. 20 (1988) 365–370.
[127] Y. Sakaguchi, M. Tokai, H. Kawada, Y. Kato, Separation of H2 and CO through poly(sulfone-diamine) membranes. III. Changes of gas permeability and membrane structure in the process of solvent removal, Polym. J. 20 (1988) 785–790.
[128] C.A. Scholes, G.Q. Chen, W.X. Tao, J. Bacus, C. Anderson, G.W. Stevens, S. E. Kentish, The effects of minor components on the gas separation performance of membrane for carbon capture, Energy Procedia 4 (2011) 681–687.
[129] Hang Zheng Chen, Tai-Shung Chung, CO_2- selective membranes for hydrogen purification and the effect of carbon monoxide (CO) on its gas separation performances, Int. J. Hydrogen Energy 37 (2012) 6001-6011.
[130] G. J. van Amerongen, The permeability of different rubbers to gases and its relation to diffusivity and solubility, J. Appl. Phys. **17** (1946) 972-985; R. M. Barrer, Viscosity of pure liquids. I. Non-polymerised fluids, Trans. Faraday Soc. **39** (1943) 48-59.
[131] S. Glasstone, K. J. Laidler and H. Eyring, The Theory of Rate Processes (McGraw-Hill Book Co., Inc., New York, 1941.
[132] R.M. Barrer, Permeability in relation to viscosity and structure of rubber, Trans. Faraday Soc. 38 (1942) 322–330.
[133] R.M. Barrer, G.J. Skirrow, Transport and equilibrium phenomena in gas elastomer systems. I. kinetic phenomena, J. Appl. Polym. Sci. 3 (1948) 549–563.
[134] D. W. Van Krevelen, Properties of Polymers: their correlation with chemical structure; their numerical estimation and prediction from additive group contribution, (Elsevier, Amsterdam, 1990).
[135] E. Ricci, M. Minelli, M.G. De Angelis, Modelling Sorption and transport of gases in polymeric membranes across different scales: a review, Membranes 12 (2022) 857.
[136] Y. Yampolskii, D. Wiley, C. Maher, Novel correlation for solubility of gases in polymers: effect of molecular surface area of gases, J. Appl. Polym. Sci. 76 (2000) 552–560.
[137] V. Teplyakov, P. Meares, Correlation aspects of the selective gas permeabilities of polymeric materials and membranes, Gas Sep. Purif. 4 (1990) 66–74.
[138] www.NIST.go.
[139] J.H. Petropoulos, Mechanisms and Theories for Sorption and Diffusion of Gases in Polymers, in D. R. Paul and Y. P. Yampolskii Eds., Polymeric Gas Separation Membranes (CRC Press, Boca Raton, FL, 1994) pp. 17-81.
[140] V. Teplyaskov, P. Maeres, Correlation aspects of the selective gas permeabilities of polymeric materials and membranes, Gas Sep. Purif. 4 (1990) 66–74.
[141] V. Bondar, B. Freeman, I. Pinnau, Gas transport properties of poly (ether-b-amide) segmented block copolymers, J Polym Sci B 38 (2000) 2051–2062.
[142] B.D. Freeman, I. Pinnau, Polymeric Membranes for Gas and Vapor Separations: Chemistry and Materials Science; B. D. Freeman and I. Pinnau, Eds.; ACS Symposium Series **733**; American Chemical Society: Washington, DC, 1999; pp 1–27.
[143] M.G. De Angelis, G.C. Sarti, Solubility of gases and liquids in glassy polymers, Annual Rev. Chem. Biomolec. Eng. 2 (2011) 97–120.
[144] G. Gee, Some thermodynamic properties of high polymers and their molecular interpretation, Q. Rev. Chem. Soc. 1 (1947) 265–298.
[145] K. Toi, G. Morel, D.R. Paul, Gas sorption and transport in poly(phenylene oxide) and comparison with other glassy polymers, J. Appl. Polym. Sci. 27 (1982) 2997–3005.
[146] G.J. van Amerongen, Influence of structure of elastomers on their permeability to gases, J. Polym. Sci 5 (1950) 307–332; R.M. Barrer, G. Skirrow, Transport and equilibrium phenomena in gas-elastomer systems, J. Polym. Sci. 3 (1948) 564–575.
[147] J.R. Park, D.R. Paul, Correlation and prediction of gas permeability in glassy polymer membrane material via a modified free volume- based group contribution method, J. Membrane Sci. 125 (1997) 23–39.
[148] V. Ryzhikh, D. Tsarev, A. Alentiev, Yu. Yampolskii, A novel method for predictions of gas permeation parameters of polymers on the basis of their chemical structure, J. Membrane Sci. 487 (2015) 189–198.
[149] M. Minelli, G.C. Sarti, Elementary prediction of gas permeability in glassy polymers, J. Membr. Sci. 521 (2017) 73–83.
[150] J.W. Barnett, C.R. Bilchak, Y. Wang, B.C. Benicewick, L.A. Murdock, T. Bereau, S. K. Kumar, Designing exceptional gas-separation polymer membranes using machine learning, Sci. Adv. 6 (2020) 4301.
[151] W.S. Ho, K. Sirkar, Membrane Handbook, Springer, New York, 1992.